THE UNIVERSITY OF ALBERTA

THE TEMPERATURE DEPENDENCE OF THE PHOTOCONDUCTIVITY OF CUPROUS OXIDE

BY

BERTRAM C. McINNIS

A THESIS

SUBMITTED TO THE FACULTY OF GRADUATE STUDIES

IN PARTIAL FULFILLMENT OF THE REQUIREMENTS FOR THE DEGREE

OF MASTER OF SCIENCE

DEPARTMENT OF PHYSICS

EDMONTON, ALBERTA

SEPTEMBER, 1963

TABLE OF CONTENTS

FIGURES

ACKNOWLEDGEMENTS

I would like to thank:

Dr. Frank L. Weichman, for introducing this subject to me and for his supervision throughout the work;

Mr. Jack Legge, for patiently doing most of the glass work required by this experiment;

Mr. Emery Fortin, for his help in the early stages of this work;

My wife, Carolyn, for her help in the preparation of this manuscript.

ABSTRACT

Experiments were conducted to determine the temperature dependence of the photoconductivity of high resistivity monocrystalline and polycrystalline cuprous oxide. It was found that the character of this temperature dependence was the same for both types of crystals. The photoconductivity displayed essentially the same temperature depencence for all incident radiation wavelengths. On the basis of a simple band model a phenomenological theory was developed which was used to analyze the observations. Qualitative agreement was obtained between the theory and the observations.

CHAPTER I: INTRODUCTION

For nearly a century it has been known that semiconductors display an increase in conductivity upon illumination. This phenomenon named photoconduction, has been observed and investigated in numerous materials. Cuprous oxide has been extensively investigated for over fifty years. The interest in this semiconductor may be attributed to the fact that it displays many electrical and optical properties such as luminescence, electroluminescence and photoconduction. Pfund (1916) was first to study the photoconduction of cuprous oxide. Since then many investigators have studied this phenomenon in cuprous oxide. A survey of the literature indicates that the majority of investigations have been oriented towards obtaining a simple band model of this semiconductor. It is the purpose of this thesis to use the simple band model, which is inherently established by the investigations, to analyze the temperature dependence of the photoconduction and thus attain some insight into the mechanisms leading to photoconduction. Fortin and Weichman (1962) have published some results of investigations on the temperature dependence of the photoconduction in cuprous oxide and it was on the basis of these results that it was decided to carry out more exhaustive studies.

CHAPTER II: APPARATUS AND EXPERIMENTAL PROCEDURE

Cuprous oxide crystals were prepared using a variation of the method used by Toth, Kilson and Trivich (1960), which is described by Fortin and Weichman (1962). Both poly and mono-crystalline samples were obtained. The crystals grown were slabs, with dimensions of about 2 x 1 x 0.05 $cm.^3$, which had smooth shiny surfaces and were transparent to red light. A layer of platinum was sputtered onto the crystal surface leaving a slit, about 0.2 cm. wide, of exposed crystal for investigation (Fig. 1 "Perspective of Sample"). Two sample holders were used. Holder A (Fig. 1) was used to measure conductivity and photoconductivity as a function of temperature in the region of 300° to -100° C. Holder B (Fig. 2) was used to measure conductivity as a function of temperature from 1000° C. to 0° C. Both holders were used to measure photoconductivity as a function of incident wavelength (response curve) at room temperature.

Holder A was designed and is extensively described by Fortin (1962). Prior to installation of samples in this holder they were outgassed under "charcoal trap" vacuum at about 1000° C. Platinum sheets mechanically pressed against the sputtered surfaces of the sample by copper plates served as electrodes. Mica sheets provided electrical insulation ($>10^{13}$ ohms) of the sample from the copper well. Temperature variation was obtained by placing an electrical heater (as shown in Fig.1) or liquid air in the copper well. This arrangement allowed sufficient thermal contact to enable a temperature of -130° C. to be reached. Due to the tendency of samples

to reduce at high temperatures, temperatures higher than about 350° C. could not be reached. A copper-constantan thermocouple spot welded to one of the platinum sheet electrodes was used for temperature measurements. This assembly together with a suitable vacuum system enabled at all attainable temperatures the maintainance of a pressure less than 10^{-6} mm. Hg. as measured by a Martin cold cathode vacuum gauge. The holder was shielded from electrical pickup by a grounded brass jacket.

Samples placed in Holder B were not outgassed before installation. For electrodes, bands of platinum were placed tightly around the sputtered parts of the sample (Fig. 2 "Perspective of Sample"). A Kanthal wound oven placed around the quartz tube was used for heating. A platinum-platinum 10% rhodium thermocouple was spot welded to one band and a platinum wire to the other. The vacuum system used with this holder maintained pressures less than 10^{-4} mm. Hg. at 1000° C. and less than 10^{-7} mm. Hg. at room temperature. Pressure was measured by a "Martir gauge" and when readings were taken, the oven was removed and the holder was shielded from electrical pickup by a grounded brass jacket. This assembly was used for conductivity measurements from 0° C. to 1000° C. and also allowed room temperature response curves to be taken after various outgassing histories.

A schematic block diagram of the general experimental layout used throughout the experiments is shown in Fig. 3. Block A represents either of the sample holders discussed above. Sample

resistance was measured using an Avometer (B) at high temperatures and a Radiometer-Copenhagen Megohmeter (B) at low temperatures. Resistances up to 10^{13} ohms could be measured. A Leeds and Northup portable potentiometer (C) measured the output of the thermocouples. The light source (D) was a Rival 355,42 watt tungsten bulb fed by a 12 volt battery in parallel with a Heathkit battery charger. A carbon rheostat was used to set the current through the lamp at a constant value of 3.5 amperes throughout the experiments. This arrangement permitted a very steady light output. The relative intensity of the source in the wavelength range from 0.4 to 2.0 microns was measured using a Golay infra-red detector. All photo-conductivity measurements were corrected to constant incident intensity by multiplying the observed response by the inverse of the intensity at any particular wavelength. The response of the sample was found to be linear for intensities used in the experiments, thus justifying this procedure. For A.C. measurements the light beam was chopped by a mechanical sector driven by a synchronous motor fed by a stabilized oscillator (E). By varying the oscillator frequency, chopping frequencies from 5 to 75 cps. could be obtained. The light beam was focussed by two cylindrical mirrors (F), on the entrance slit of a Leiss quartz double monochromator (G). Analyzed by two prisms in series the light came out of the exit slit of the monochromator with a spectral purity of about 3% for the wavelengths used. The output lying in the wavelength range of 0.4 to 2 microns was focussed onthe exposed portion of the sample. The circuit (H) used for

photoconductivity measurements is shown in Fig. 4. A known resistance (load resistance) was placed in series with the sample and a D.C. supply was connected across the two. The on-off incident light beam caused the sample resistance to vary thus varying the current and voltages throughout the circuit. Voltage variation at the floating end of the load resistance was used as a direct measure of the photocurrent.

In the following the photocurrent will be defined as the current passing through the sample when exposed to light minus the current passing through the sample when in complete darkness. Let the applied voltage be V, the load resistance be R, the sample resistance be R_s, the current be I and the voltage at the floating end of R be V_o. The subscript D will refer to a particular variable when the light is off and the subscript L will refer to the variable when the light is on. By definition;

$$\Delta I = I_L - I_D \text{ ; where } \Delta I \text{ is the photocurrent.}$$

Thus, $$\Delta I = V(1/R_{SL} + R) - 1(R_{SD} + R)).$$

But: $$V_{OD} = I_D R = VR/(R_{SD} + R),$$

and $$V_{OL} = I_L R = VR/(R_{SL} + R),$$

therefore; $$V_{OL} - V_{OD} = VR(1/(R_{SL} + R) - 1/(R_{SD} + R)),$$

or $$V_{OL} - V_{OD} = R\,\Delta I.$$

Therefore, using this arrangement the photocurrent can be measured directly.

A high imput impedance amplifier (Fig. 5), was used to detect the voltage at the floating end of R. This arrangement had two advantages over measuring the photocurrent directly across the sample:

1. A smaller input impedance amplifier could be used and
2. The input impedance to the amplifier remains constant over relatively wide temperature ranges.

The line from the sample to the amplifier was double shielded with the outside shield being grounded. The inside shield floated at D.C. voltage which was fed back by the amplifier and was proportional to the input signal. This helped cancel stray capacitance. All other lines were provided with grounded shields. Tests showed that the amplifier was linear from 100 cps. to D.C., introduced no distortion at input impedances of up to 100 megohms, had an amplification factor of about 4, and had a rise time of 0.05 milliseconds. The output of the amplifier was fed to a Hewlett-Packard vacuum tube voltmeter (I) and to a 502 Dual Beam Tektronix Oscilloscope (J) for measurements. Using the oscilloscope on X-Y display and feeding a signal from an oscillator (K) onto one display and the signal from the amplifier onto the other, the chopping frequency could be easily measured.

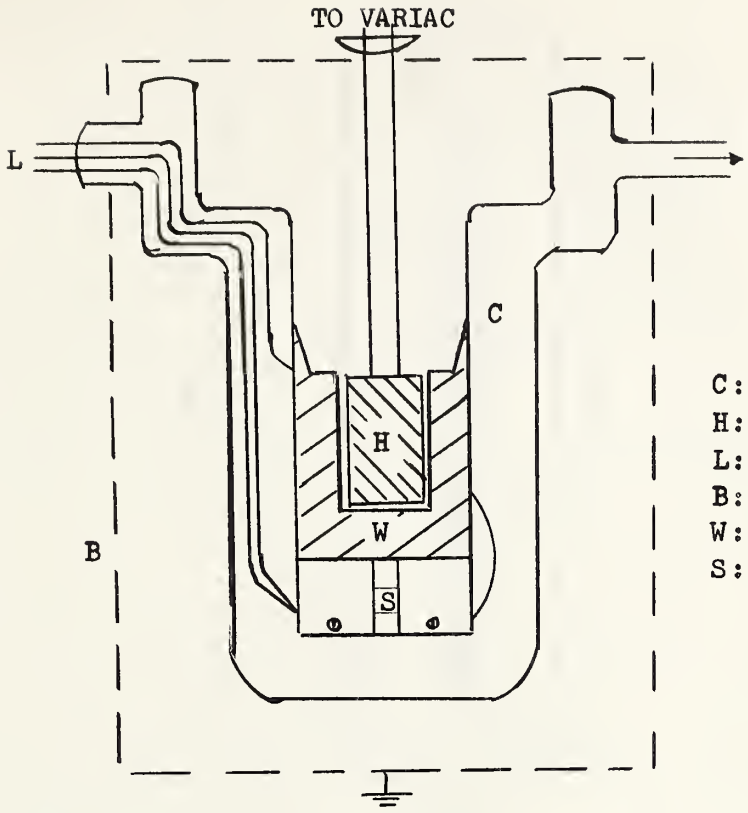

C: COPPER-TO-PYREX SEAL
H: HEATER
L: LEADS
B: SHIELD
W: COPPER WELL
S: SAMPLE

CROSS-SECTIONAL VIEW

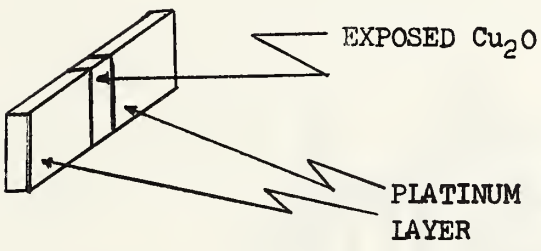

PERSPECTIVE OF SAMPLE

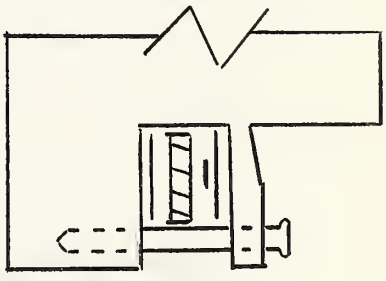

FROM LEFT TO RIGHT: COPPER-MICA-SAMPLE-ELECTRODES-MICA-COPPER
VICINITY OF SAMPLE (SIDE VIEW)

FIGURE 1: SAMPLE HOLDER A

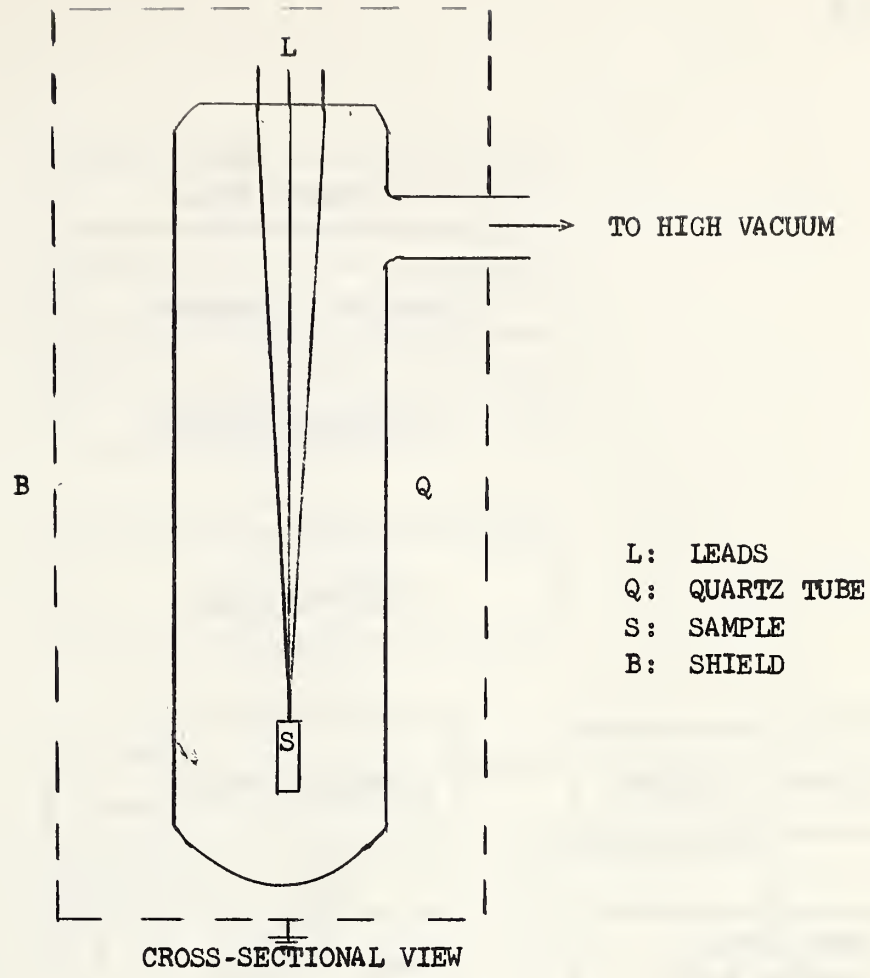

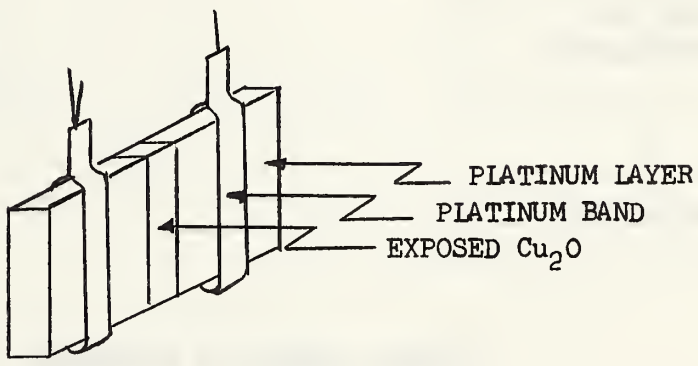

FIGURE 2: SAMPLE HOLDER B

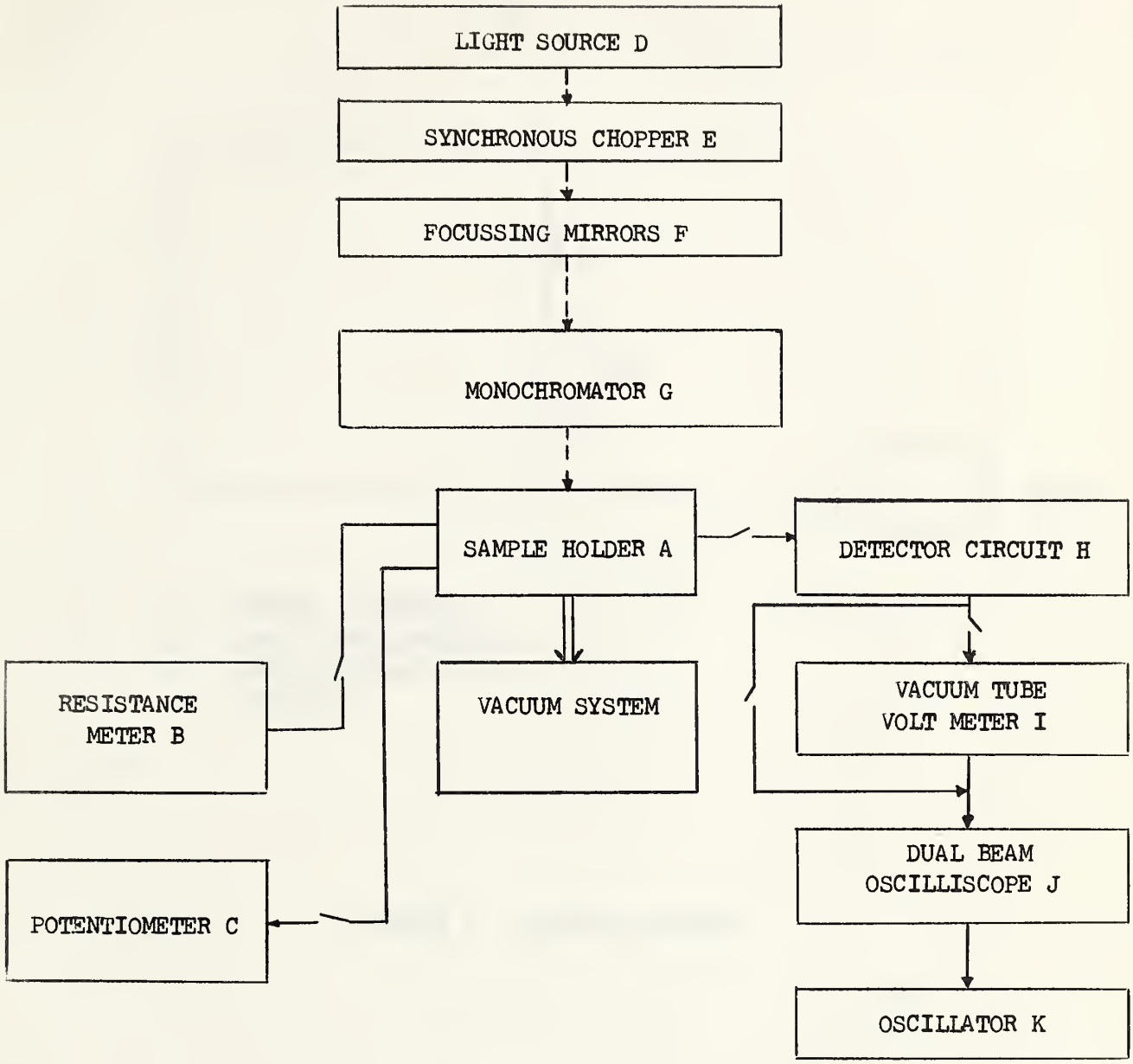

FIGURE 3: SCHEMATIC OF GENERAL LAYOUT

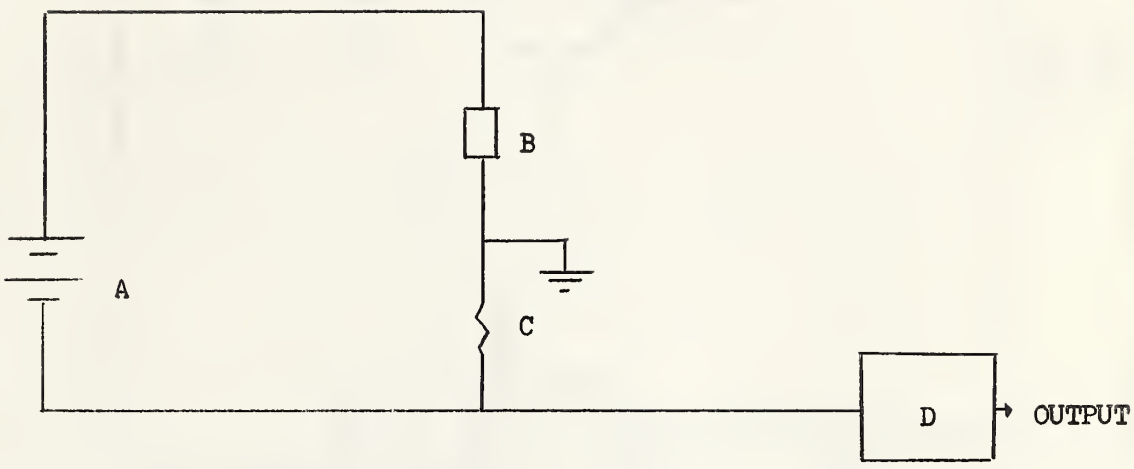

A: BATTERY (VOLTAGE=V)
B: SAMPLE (RESISTANCE=R_S)
C: LOAD RESISTANCE = R
D: AMPLIFIER

FIGURE 4: DETECTOR CIRCUIT

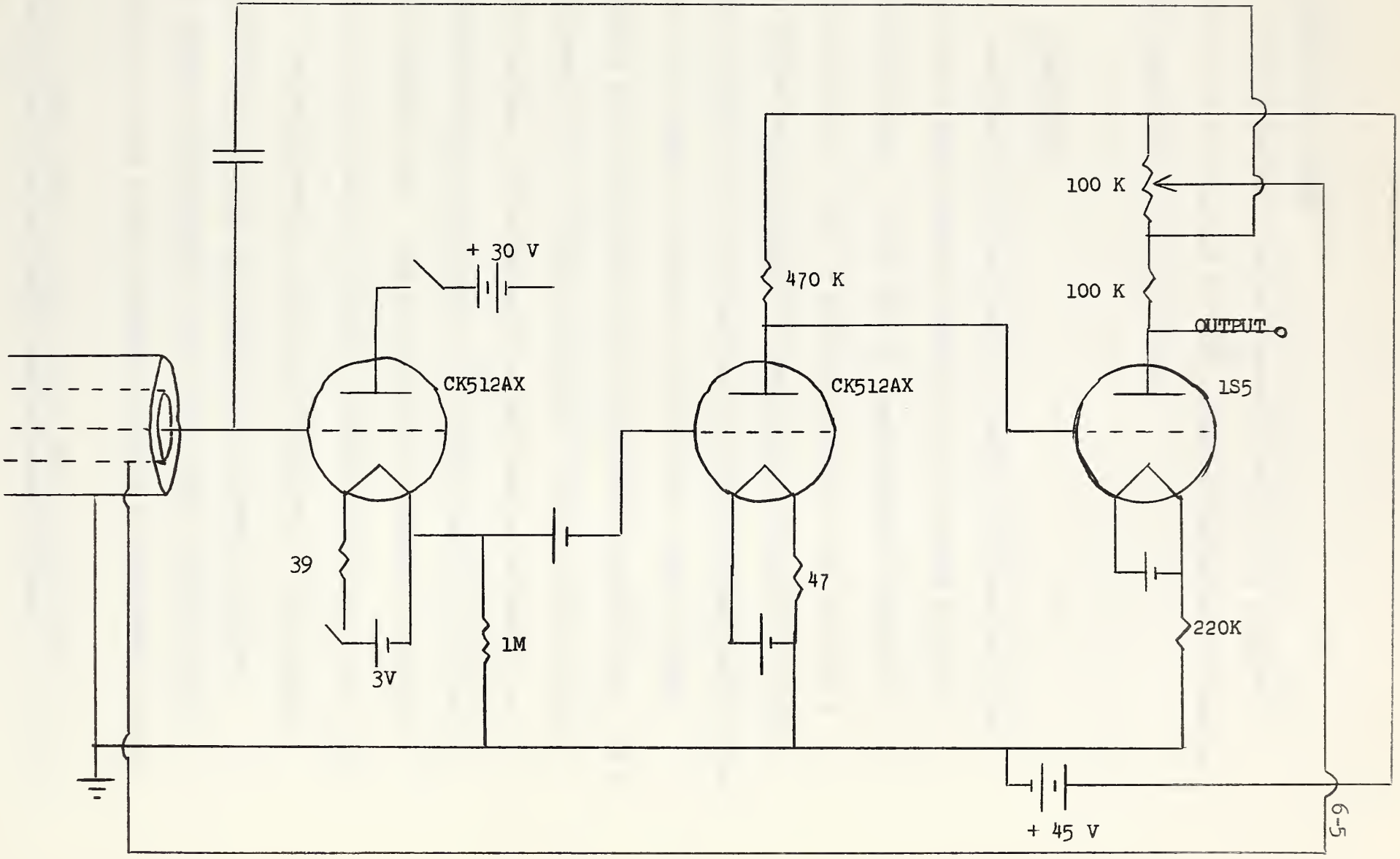

FIGURE 5: AMPLIFIER

CHAPTER III: THEORY

The following is not an exhaustive study of the pertinent theory, but is presented for the purpose of elucidation of concepts and familiarization with terminology.

A. CONDUCTIVITY

According to the band theory of solids, electrons can exist in bands of quasi-continuous energy levels separated by gaps of forbidden energy. In the case of a semiconducting crystal, at absolute zero all bands of allowed energy up to and including a particular band are filled.(1) The highest (energy wise) filled band is called the valence band and all bands of allowed energy higher than it are empty at absolute zero. The first band of allowed energies above the valence band is called the conduction band. For a semiconductor the forbidden energy gap is such that above absolute zero electrons can be thermally excited from the valence to the conduction band leaving holes in the valence band and electrons in the conduction band. Upon application of an electric field both electrons and holes will be able to migrate through the crystal, via their respective bands, giving rise to conduction. The conduction resulting from band to band transitions is known as intrinsic. In compound semiconductors, like cuprous oxide, permitted energy levels may exist in the forbidden gap due to a stoichiometric excess

(1) An energy level is called "filled" when occupied by an electron and is called "empty" when occupied by a hole.

of one constituent element. These levels fall into a general category termed impurity levels. Conduction, known as extrinsic, may also occur due to band, to or from impurity level, transitions. Two types of impurities may occur resulting in two types of extrinsic conduction. They are: the donor type of impurity allowing transitions of electrons from the impurity level to the conduction band giving rise to electron or n-type conductivity; the acceptor type of impurity allowing transitions of holes from the impurity level to the valence band giving rise to hole or p-type conductivity. Inter-impurity level transitions are possible but are expected to be ineffective if only low concentrations of impurities are present. Most semiconductors are extrinsic at room temperature and lower.

At any given temperature an equilibrium is established between the thermal excitation and recombination of charge carriers resulting in an equilibrium concentration of charge carriers being present in the conduction and/or valence band. The conduction arising from this process is termed "dark conduction". The temperature dependence of the conductivity of a semiconductor can be shown to be of the form[2];

$$\sigma = \sum_{i=1}^{n} A_i \exp(-E_i/2kT) \qquad (1)$$

for a semiconductor with n-1 impurity levels. If each impurity level is such that the number of available charge carriers is larger than the number of impurity levels to or from which the bulk of the excitation is occuring then[3];

(2) M.F. Mott and R.W. Gurney. Electronic Processes in Ionic Crystals. Oxford: 1948, pages 156 to 160.

(3) Ibid.

$$E_i > E_{i+1} \text{ and } A_i > A_{i+1}$$

E_1 is the "activation energy" for intrinsic conductivity and $E_2 \ldots . E_n$ are the activation energies for extrinsic conductivity. Each of these terms in equation (1) will dominate in a particular temperature region. A plot of log conductivity versus inverse absolute temperature will yield a series of straight lines whose slopes are the activation energies. If in a particular region an activation energy, E_i, is obtained, then in this region the conductivity is predominantly due to transitions over an energy gap of E_i . The above statement is subject to the restriction that the number of available charge carriers is greater than that number of available states[4]. Thus from conductivity versus temperature measurements a picture of the relative energy level spacing may be determined.

B. PHOTOCONDUCTIVITY

In numerous semiconductors it has been observed that electrical conduction increases upon illumination by electromagnetic radiation. This phenomenon is called photoconduction and it implies that illumination increases the free charge carrier concentration. The definition of photocurrent (see Chapter II, page 5) is essentially: "that current which is produced by optically excited carriers". Since conductivity is proportional to free charge carrier concentration

(4) Ibid.

the terms "photocurrent" and "optically excited free charge carrier concentration" will be used interchangeably in the following.

On the basis of the simple band model discussed above, three modes of excitation are possible. These are "band to band", "band to or from impurity level" and "impurity level to impurity level" transitions. For low impurity concentration semiconductors the last mode is expected to be least effective. In the first of these modes the radiation excites electrons from the valence to the conduction band creating free holes in the valence band and free electrons in the conduction band. Each excitation creates a free electron-hole pair. In the second of these modes the incident radiation may excite electrons from impurity levels to the conduction band resulting in free electrons in the conduction band or it may excite electrons from valence band to impurity levels resulting in free holes in the valence band. Here each excitation produces only one free carrier. In the third mode the radiation excites electrons from one impurity level to a higher lying one. This mode does not give rise to free carriers directly but due to the subsequent thermal redistribution, free carriers are created. It will be found convenient to define the following terms. "Bound State" refers to a state or level in which the resident particle is unable to migrate spatially. "Free State" refers to a state in which the resident particle is free to migrate spatially. Therefore, filled or empty bands represent bound states, while partially filled bands contain

free states and impurity levels, whether filled or empty, are bound states.

Now consider a semiconductor illuminated by radiation. A steady influx of radiation is present, thus, via excitation the free carrier density will initially be increasing in time. If the illumination is interrupted the electrons (holes) will undergo transitions to bound states in order to reestablish thermal equilibrium. This process is called recombination. Under a steady influx of radiation the process of excitation will tend to increase the number of free carriers while the process of recombination will tend to decrease the number of free carriers. It is evident that an equilibrium state will be obtained in which the rate of excitation equals the rate of recombination. This equilibrium state will be shifted away from the thermal equilibrium state in such a way as to increase the steady state number of free carriers. On the basis of the simple band model, three modes of recombination are possible. These are: recombination by transitions of electrons from the conduction to the valence band (direct recombination), recombination by transitions of electrons (holes) from the conduction (valence) band to bound states (bound state recombination) and the third possibility is recombination via impurity level to impurity level transitions which decrease the carrier concentration upon thermal redistribution. This third mode could also be called bound state recombination. For the latter two of these modes, the recombination is said "to occur at the bound state". The first mode occurs at the valence or conduction band, depending on whether electrons or holes are considered

as making the transitions respectively. In the following it will be assumed that the influential mode of recombination is bound state recombination. Bound states may be divided into two categories: those near the conduction band (valence band) from which an electron (hole) is more likely to be thermally re-excited into the conduction band (valence band) than to recombine or be captured by a free hole (electron), and those more remote from the conduction band (valence band) in which an electron (hole) is more likely to recombine with or be captured by a free hole (electron) than to be thermally re-excited into the conduction band (valence band). The first of these are called "trapping states" and are located near the band edges[5]. The second of these are called "ground states" [6] and are remote from the band edges. The connotation of ground state is that the optically excited electron (hole) has completed its free life history when captured by a ground state level. The lifetime of a free carrier is the total time spent in a free state (conduction band for electrons and valence band for holes). It is the central parameter upon which the photocurrent depends. The occupation of the trapping states is determined by thermal exchange of carriers with the free states of their respective band edges. Thus these states tend to be in thermal equilibrium with their free carriers and will not affect the magnitude of the steady

(5) Trapping states near the conduction band are called electron traps and trapping states near the valence band are called hole traps.
(6) A detailed discussion of ground and trapping states as they relate to photoconductivity is given by Rose (1954) (1955).

state photocurrent, but they do have a marked effect on the time required to set up the steady state photocurrent (rise time), and the time required for the photocurrent to dissipate (decay time) when optical excitation is interrupted. Since the incident radiation in building up the photocurrent must also fill the trapping states, the ratio of the rise time to the free carrier lifetime is expected to be of the order of the ratio of trapped to free carriers. Similarly upon decay the trapping states must be emptied, thus the ratio of the decay time to the carrier lifetime is expected to be of the order of the ratio of trapped to free carriers. Thus both the rise and decay times are larger than the lifetime of the free carriers since the number of trapped carriers is larger than the number of free carriers. Also since the decay of the photocurrent is dependent upon ground state capture, whereas, excitation is direct, the decay time is expected to be longer than the rise time. Thus trapping states determine the response times of the semiconductor. Ground states determine the lifetime of the free carriers and thus the magnitude of the photocurrent since recombination must occur through these states. For a particular sample of a semiconducting material in a fixed environment, the external variables which can be used to probe the mechanisms of photoconduction are incident radiation wavelength (energy), incident radiation, intensity, and temperature. In order to discuss the variation of the photocurrent with incident radiation energy an extremely simplified model is taken. A set of ground states, G, at an energy, E_2 above

above the valence band, V, is postulated. The difference in energy from the top of the valence band to the bottom of the conduction band, C, is E_1. Let E be the energy of incident radiation. For E greater than E_1, V-C [7] transitions are dominant and the photocurrent is constant. Consider the variation for decreasing E or increasing wavelength. For E of the order of E_1 it is expected that the photocurrent will decrease rapidly. In the region $E_1 > E > E_2$ the photocurrent will be predominantly due to V-G transitions and will be constant. As E becomes of the order of E_2 the photocurrent will again drop rapidly. Thus the photocurrent should appear as a set of decreasing steps. The photocurrent due to V-G transitions is smaller than the photocurrent due to V-C transitions because of the smaller number of available states for the V-G transitions. Moss (1952) has shown that for a monatomic solid the photocurrent should be constant for $E > E_1$ dropping off exponentially as E becomes of the order of E_1 and that the value of E at which point the photocurrent has fallen to one half its maximum value should be E_1 ($\lambda_{\frac{1}{2}}$ concept). It is generally assumed that this result may be extended to poly-atomic solids and that it may also be extended to the range of E of the order of E_2. Thus the band gap and impurity level spacing can be determined from the response curve of a semiconductor. Photoconductive response data generally reveal that a low continuous background response is present with a few peaks. This indicates that

(7) Henceforth; X-Y transitions mean transitions from the X level or band to the Y level or band by electrons.

in the forbidden gap a low continuous background density of levels with a few high density levels are present.

Now consider the variation of the photocurrent with incident intensity. For this purpose the same model as above is used except that a set of electron traps has been added such that the photocurrent is carried predominantly by holes, since this is believed to be the situation for cuprous oxide. Because the effect of trapping on the magnitude of the photocurrent is small, it will be neglected in the rate equation. Let;

L = the incident light intensity
A = rate of thermal excitation from valence band
R = probability of optical excitation
D = the recombination coefficient.

Assume the mode of excitation is band to band and that recombination may be characterized by one coefficient. Let M be the density of impurity levels G, and P be the density of holes in the valence band with P_o the hole density at thermal equilibrium. Numerous authors have discussed this model on theoretical basis (See Moss, 1952). Under these conditions the rate equation for build up is;

$$dP/dt = A + LR - DP(P + M). \qquad (2)$$

When L = 0 and thermal equilibrium is achieved; $dP/dt = 0$,

$P = P_o$ and $A = DP_o(P_o + M)$. Let $\Delta P = P - P_o$;

therefore; $\frac{d\Delta P}{dt} = \frac{dP}{dt}$ AND;

$$dP/dt = LR - D\Delta P(\Delta P + X) \qquad (3)$$

where $X = M + 2P_o$. Under steady state conditions let $\Delta P = \Delta P_o$, therefore;

$$\Delta P_o(\Delta P_o + X) = LR/D \ . \qquad (4)$$

Consider two cases:

CASE 1: For $\Delta P_o >> X$ or high light intensity;

$(\Delta P_o)^2 = LR/D$ or,

$$\Delta P_o \propto L^{1/2} \quad , \quad (5)$$

and the photocurrent increases as the square root of the light intensity.

CASE 2: For $\Delta P_o << X$ or low light intensities;

$\Delta P_o = LR/XD$ or,

$$\Delta P_o \propto L \quad , \quad (6)$$

and the photocurrent increases linearly with incident light intensity.

At high light intensities the mode of recombination is band to band while at low light intensities the mode is bound state, thus for a linear dependence of photocurrent on light intensity the recombination is mainly due to bound states.

In considering the temperature dependence of the photocurrent the same model as above is used. Integration of equation (3) yields:

$$\frac{\Delta P_o - \Delta P}{\Delta P_o + \Delta P + X} = \frac{\Delta P_o}{\Delta P_o + X} \exp\left(-D(X + 2\Delta P_o)t\right) \quad (7)$$

and in the low light intensity approximation ($\Delta P < \Delta P_o << X$) equation (7) becomes:

$$\Delta P = \Delta P_o(1 - \exp(-DXt)) \quad (8)$$

which in the steady states ($t = \infty$) yields the photocurrent as $\Delta P = \Delta P_o$ which is of course the result obtained in Case 2 above. Thus the steady state charge carrier density increase is given by;

$$\Delta P_o = (LR/D) \,/(M + 2P_o) \quad . \tag{9}$$

The increase in conductivity $\Delta\sigma$ arising from a charge carrier density increase of ΔP is given by;

$\Delta\sigma = \Delta P\, e\, u$; where u is the carrier mobility and e the electronic charge. If a uniform electric field $\mathcal{E}$, is applied, then the photocurrent $\Delta I''$ is given by; $\Delta I'' = \mathcal{E}\, \Delta P\, e\, u\, A$, where A is the cross-sectional area of the sample. Let the photocurrent be given in terms of current per unit area, $\Delta I'$. Then;

$$\Delta I' = (e\, \mathcal{E}\, u\, R\, L/D)/(M + 2P_o) \quad .$$

Since all photocurrent measurements have been normalized to a flat intensity spectrum, the value plotted in this thesis and called photocurrent is ΔI where; $\Delta I = \Delta I'/L$.

Thus; $$\Delta I \propto (uR/D)/(M + 2P_o) \tag{10}$$

and the temperature dependence of ΔI will arise out of the temperature dependence of u, R, D, and P_o. On the basis of the model being used the temperature dependence of P_o is given by;

$$P_o = A_1 \exp(-E_1/2kT) + A_2 \exp(-E_2/2kT)$$

where T is the absolute temperature and A_1 and A_2 are constants.

In the above derivation, the conduction band with its associated traps may be replaced by a single impurity level, leaving the essentials of the derivation unchanged. Thus the form of the photocurrent will be the same. For this new model R and D will refer to different processes and ΔI will be given by;

$$\Delta I = (uR'D')/(M' + 2P_o) \tag{11}$$

where the prime indicates that the symbols refer to different

processes. This implies that the photocurrent will have the same general temperature dependent features independent of the incident radiation wavelength.

The model may now be replaced by a model that is the same except that a relatively dense impurity level is placed very near the band. Excitation at a particular wavelength may now occur via two processes: excitation from the valence band as before or excitation from this impurity level. Since the impurity level is close to the valence band, they are in thermal equilibrium and excitation from this impurity level will increase the density of charge carriers in the valence band. Thus it may occur that two processes are competing for excitation. It is not unreasonable to expect that the photocurrent arising from excitation from this impurity level will have the same general temperature dependence features as given in equation (10) with R and B different because they refer to different processes. Thus the dependence of the photocurrent may be written as:

$$\Delta I = (uR_1/D_1)/(M_1 + 2P_o) + (uR_2/D_2)/(M_2 + 2P_o) \qquad (12)$$

where each term refers to a particular process. They have been written separately to indicate that the response times of these processes may be markedly different. It is also expected that the response times of these processes will be temperature dependent. As can be seen from equation (8), the rise time, T_R, of the process it refers to is given by;

$$T_R = 1/D(M + 2P_o).$$

Consider the term $(uR/D)/(M + 2P_o)$. u is expected to increase slightly with decreasing temperature. Both R and D are expected to decrease upon decreasing temperature. For simplicity assume the uR/D may be represented as;

$uR/D \propto \exp(-E_o/kT)$ and consider the temperature region in which $P_o = A_2 E^{-E_2/2kT}$. Thus;

$$\Delta I \propto \frac{\exp(-E_o/kT)}{M + A_2 \exp(-E_2/2kT)} \quad . \tag{13}$$

For low enough temperatures $M >> P_o$, thus $\Delta I \propto \exp(-E_o/kT)$ and at low temperatures ΔI decreases exponentially with inverse temperature. At high enough temperatures $P_o >> M$ and $P \propto \exp(-E_2/2kT)$. Thus; $\Delta I \propto \exp((E_2/2 - E_o)/kT)$ and assuming $E_2/2 - E_o$ is positive, the photocurrent will increase exponentially with temperature. If competing processes are present they will both have the same temperature dependence as above but at different levels of magnitude and in different temperature ranges and with different E_i. For a particular process the photocurrents' temperature dependence is exponential at high temperatures, changing over to an exponential behavior at low temperatures with a different exponent. Since when $M >> P_o$ the exponent is positive and when $M << P_o$ the exponent is negative there arises the possibility of defining a critical temperature as T_c given by the condition;

$$E_o M = P_o(E_2/2 - E_o) \tag{14}$$

at which point the photocurrent is a maximum. This gives a critical temperature of;

$$T_c = \frac{E_2}{2kLn(A(E_2/2 - E_o)/ME_o)} \quad . \qquad (15)$$

As in all experiments one must be aware of the effect on the results of the experimental technique. In the case of results taken in this experiment it became increasingly apparent as the work was carried through that the A.C. method may have a marked effect on the results.

C. EFFECT OF CHOPPING FREQUENCY ON THE OBSERVED PHOTOCURRENT

Assume that at any temperature and incident wavelength that there are competing processes present. These processes will be referred to as the "A" and "K" processes. Process A is assumed always larger than process K for steady state. The response time of process K is always much smaller than process A, that is K is very fast compared to A. Let the chopping frequency be $1/2t_o$, thus the incident intensity as a function of time is a square wave as shown in Fig. 6a. Let the response times of the fast process be T_R^K and T_D^K, where R refers to the rise time and D to the decay time and let the response times of the slow process be T_R^A and T_D^A. These are assumed to have magnitudes such that; $T_R^K \leq T_D^K << T_R^A \leq T_D^A$, and it is assumed that t_o, the chopping time, is of the order of the response times of the slow process. Thus with respect to the chopping time, the K process will appear as a square wave (See Fig. 6b, "Fast: A.C."). The sum of the A and K processes is shown in Fig. 6b as the curve marked "Fast + Slow: A.C.".

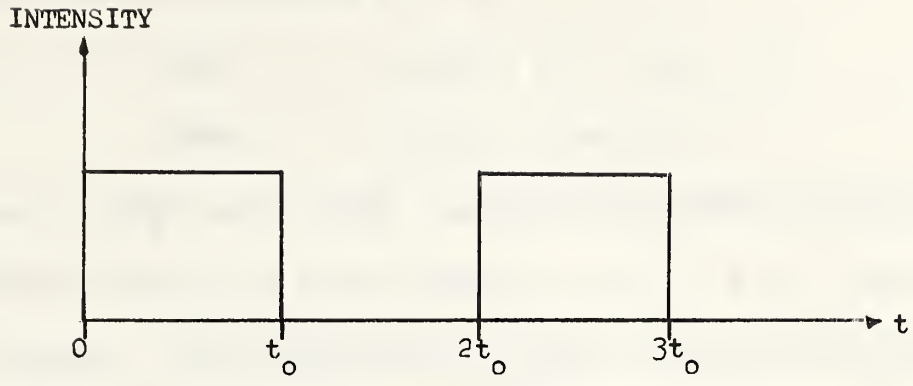

FIGURE: 6a

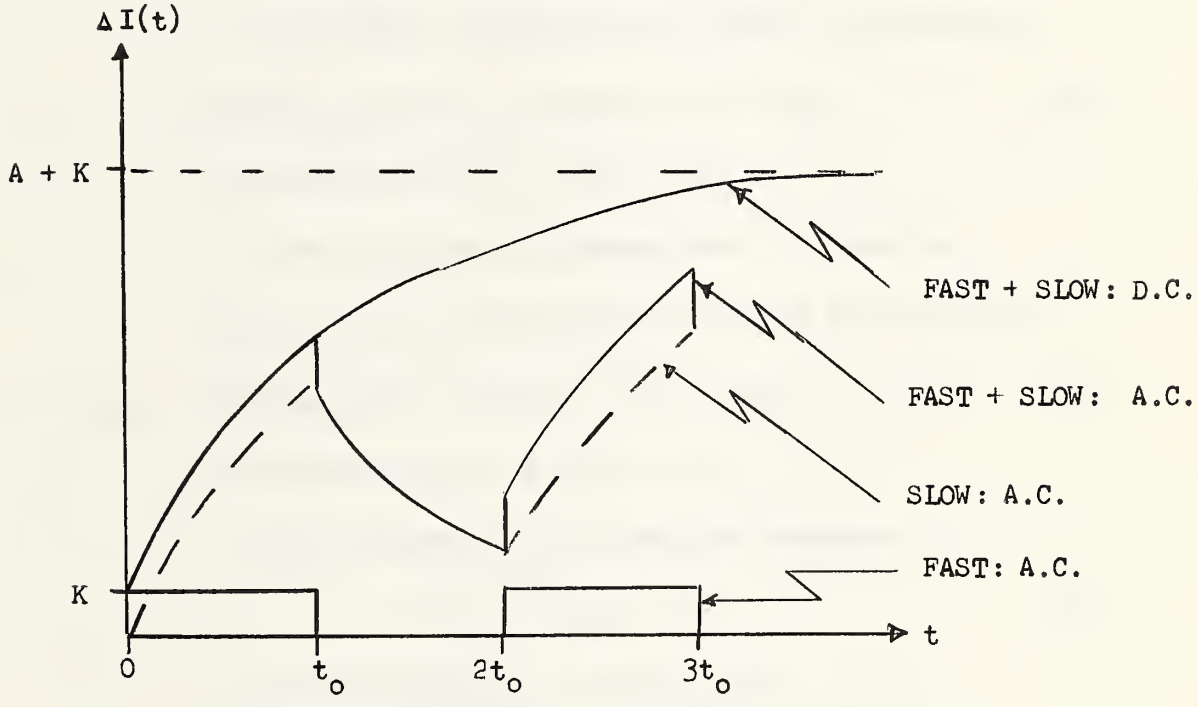

FIGURE: 6b

Consider the time dependence of the slow process A. Assume[8] that it may be represented as:

$$\text{RISE} \qquad \Delta I_R(t) = A(1 - \exp(- xt)) \tag{16}$$

$$\text{DECAY} \qquad \Delta I_D(t) = A \exp(- yt) \tag{17}$$

where $x = 1/T_R^A$ and $y = 1/T_D^A$. Let the photocurrent be denoted by a subscript n when t is in the range $(n - 1)t_o \leq t \leq nt_o$, where n is integral. The photocurrent will have a discontinuous slope at the points nt_o. The boundary conditions to be used are:

1. From any value of photocurrent, F, when the light is interrupted, the photocurrent decays according to;

$$\frac{d}{dt} \Delta I_{D,n+1}(t) = - yF \exp(- y(t - nt_o)) \tag{18}$$

in the region $nt_o \leq t \leq (n + 1)t_o$.

2. From any value of photocurrent, R, when the light is put on the photocurrent rises according to;

$$\frac{d}{dt} \Delta I_{R,n+1}(t) = xR \exp(- x(t - nt_o)) \tag{19}$$

in the region $nt_o \leq t \leq (n + 1)t_o$.

3. When the sample is in complete darkness;

$$\Delta I_{D,n}(t = \infty) = 0 \tag{20}$$

4. When the sample is in the light;

$$\Delta I_{R,n}(t = \infty) = A \tag{21}$$

Applying these conditions to the successive time regions, $(0, t_o)$ $(t_o, 2t_o)$ etc., and using induction it may easily be shown that;

(8) This assumption is substantiated by numerous discussions on the theory of photoconduction. See for instance, Moss (1952), also see equation 8, page 16.

$$\Delta I_n(t) = \Delta I_{n-1}((n-1)t_o)\exp(-(\frac{1-(-1)^n}{2}x + \frac{1+(-1)^n}{2}y)(t-(n-1)t_o)) + \frac{1-(-1)^n}{2}\Delta I_1(t-(n-1)t_o) \quad (22)$$

where $\Delta I_1(t) = A(1-\exp(-xt))$ and $n=1,2,3,\ldots$.

When n is even the photocurrent is decaying and when n is odd the photocurrent is rising. The condition of continuity may be stated as:

$$\Delta I_n((n-1)t_o) = \Delta I_{n-1}((n-1)t_o) \quad . \quad (23)$$

Equation (22) yields:

$$\Delta I_n(nt_o) = \Delta I_{n-1}((n-1)t_o)\exp(-(\frac{1-(-1)^n}{2}x + \frac{1+(-1)^n}{2}y)t_o) + \frac{1-(-1)^n}{2}\Delta I_1(t_o) \quad , \quad (24)$$

and;

$$\Delta I_{n-1}((n-1)t_o) = \Delta I_{n-2}((n-2)t_o)\exp(-(\frac{1-(-1)^{n-1}}{2}x + \frac{1+(-1)^{n-1}}{2}y)t_o) + \frac{1-(-1)^{n-1}}{}\Delta I_1(t_o) \quad . \quad (25)$$

But under steady state conditions ($t = \infty$);

$$\Delta I_n(nt_o) = \Delta I_{n-1}((n-2)t_o) \quad . \quad (26)$$

Substitution of(23) and (26) into (24) and (25) allows (24) and (25) to be written in terms of $\Delta I_n(nt_o)$ and $\Delta I_n((n-1)t_o)$ and thus explicit solutions for $\Delta I_n(nt_o)$ and $\Delta I_n((n-1)t_o)$ may be obtained as;

$$\Delta I_n(nt_o) = A(1-\exp(-xt_o))/(1-\exp(-(x+y)t_o)) \quad ,$$

and $$\Delta I_n((n-1)t_o) = A(1-\exp(-xt_o))(\exp(-yt_o))/(1-\exp(-(x+y)t_o)) \quad .$$

Thus the photocurrent that is measured, ΔI_M, which is given by $\Delta I_M = \Delta I_n(nt_o) - \Delta I_n((n-1)t_o)$, may be written as;

$$\Delta I_M = A\,\frac{(1-\exp(-xt_o))(1-\exp(-yt_o))}{(1-\exp(-(x+y)t_o))} \quad . \quad (27)$$

Under the conditions of low light intensity it may be assumed that the competing processes act independently and thus the total photocurrent, ΔI, is given as:

$$\Delta I = K + \Delta I_M \quad . \tag{28}$$

It should also be noted here that if $t_o << 1/x$ and of the order of the response times of the fast process, then:

$$\Delta I = K \frac{(1-\exp(-t_o/T_R^K))(1-\exp(-t_o/T_D^K))}{(1-\exp(-(1/T_R^K + 1/T_D^K)t_o))} \quad . \tag{29}$$

In order to simplify equation (28) consider the approximation that $T_R^A = T_D^A = T_A$ is implemented. Under this condition;

$$\Delta I = K + A \frac{(1-\exp(-t_o/T_A))}{(1+\exp(-t_o/T_A))} \quad . \tag{30}$$

For further simplification let $T_A >> t_o$ and consider the first order approximation of (30) which gives;

$$\Delta I = K + \frac{A\ t_o}{2\ T_A} \quad . \tag{31}$$

Equation (31) should hold when T_A is large compared to t_o and t_o is large compared to response times of the fast process. If equation (29) is applicable and approximations similar to those leading to equation (31) are used, ΔI is given as:

$$\Delta I = \frac{K\ t_o}{2\ T_K} \quad . \tag{32}$$

K and A are the steady state values of the photocurrent resulting from the fast and slow processes respectively, thus:

$$\begin{aligned} K &= K(T,\lambda) \\ A &= A(T,\lambda) \ , \end{aligned} \tag{33}$$

where T is the absolute temperature and λ the incident wavelength. Thus depending on the values of T_A, T_K and t_o, one may qualitatively

express the temperature dependence in regions as;

1. $t_o >> T_A$; $\Delta I = K + A$

2. $T_A >> t_o >> T_K$; $\Delta I = K + \frac{A t_o}{2 T_A}$

3. $T_A >>> t_o >> T_K$; $\Delta I = K$

4. $T_K >> t_o$; $\Delta I = \frac{K t_o}{2 T_K}$

with transition regions between these regions. There is evidence, Ryvkin (1949), that in Cu_2O the response time increases exponentially with inverse temperature, thus if it is assumed that;

$$T_A = T_{oA} \exp(E_A/kT) \text{ and } T_K = T_{oK} \exp(E_K/kT) \qquad (34)$$

the qualitative regions above may be rewritten as:

1. $\Delta I = K + A$

2. $\Delta I = K + A \frac{t_o}{2 T_{oA}} \exp(-E_A/kT)$

3. $\Delta I = K$

4. $\Delta I = \frac{K t_o}{2 T_{oK}} \exp(-E_K/kT)$

For a fixed wavelength both K and A will have a temperature dependence of the form given by equation (24), or with appropriate approximations, equation (27). Thus a complicated temperature dependence of the photocurrent may be expected. A number of ways in which the photocurrent may vary can be envisioned on the basis of the above discussed variables. A few general remarks may be made. It is likely that at high temperatures the photocurrent will increase exponentially with inverse temperature reaching a maximum. If the response time becomes of the order of the chopping time

of one process the A.C. measured photocurrent will decrease faster with decreasing inverse temperature than the D.C. measured photocurrent.

The concepts developed in this chapter will be used to analyze the observed temperature dependence of the photocurrent.

CHAPTER IV: OBSERVATIONS AND DISCUSSION

A. CONDUCTIVITY VERSUS INVERSE ABSOLUTE TEMPERATURE (CONDUCTION CURVES)

These measurements were carried out in order to characterize the samples and to provide a comparison of their behavior with the behavior of samples studied by previous investigators.

Fig. 7 shows typical conductivity curves obtained from samples installed in holder A. After preparation these samples were outgassed under charcoal trap vacuum at 1000°C and installed in the holder. They were then annealed at 300°C under high vacuum (10^{-7}mm. hg.). For this thermal history the polycrystalline samples showed only one distinct region (one slope) while the monocrystalline samples showed two distinct regions (two slopes) in the temperature region of 500°K to 200°K. The slopes of the curves for monocrystalline samples were steeper than those for polycrystalline samples indicating that the impurity levels for monocrystalline samples lie higher above the valence band than those for polycrystalline samples.

Figures 8a and 8b show typical conductivity curves obtained from samples installed in holder B. After preparation these samples were installed in the holder and then annealed at 1000°C under high vacuum (10^{-5} mm. hg.). Polycrystalline samples with this thermal history showed three distinct regions in the temperature range from 1000°K to 250°K. The monocrystalline samples showed two regions. Again the slopes for monocrystalline samples at corresponding temperatures were steeper than those for polycrystalline samples.

If in the region of the conductivity curves where the slope is the steepest the conductivity is assumed intrinsic, then for monocrystalline samples intrinsic conductivity sets in at lower temperatures than for polycrystalline samples.

Although the conductivity curves vary from sample to sample and with thermal history, two general statements may be made:

1. In the temperature region under investigation (1000°K to 200°K), the conductivity curves for both poly- and monocrystalline samples show three regions indicating the conductivity may be expressed as;

$$\sigma = \sum_{i=1}^{3} A_i \exp(-E_i/2kT).$$

2. Monocrystalline samples have lower conductivities and higher lying impurity levels than polycrystalline samples.

The interpretation of these data in terms of a simple band model would indicate impurity levels lying from 0.6 e.v. to 1.0 e.v. above the valence band for polycrystalline samples, and impurity levels lying from 0.8 e.v. to 1.4 e.v. above the valence band for monocrystalline samples, with a band gap in the region of 1.8 e.v. to 1.9 e.v.. These impurity levels are usually attributed to excess oxygen or deficient copper existent in the lattice (See for example O'Keefe and Moore, 1961). Fortin(1962) has given a survey of the pertinent literature and the concensus of this literature is compatible with the observations presented here.

The main conclusion drawn from this data is that impurity levels

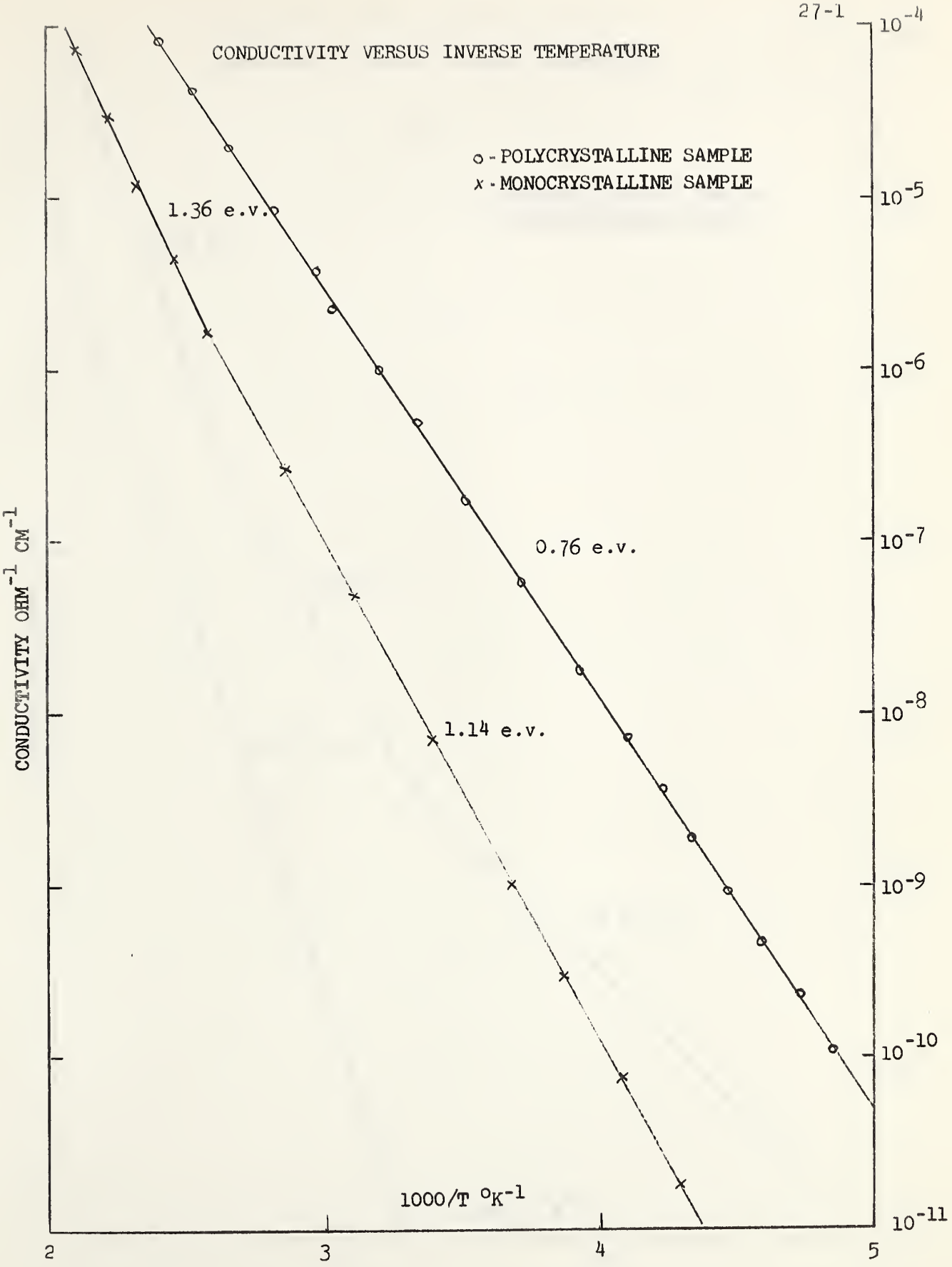

FIGURE 7: CONDUCTIVITY CURVES

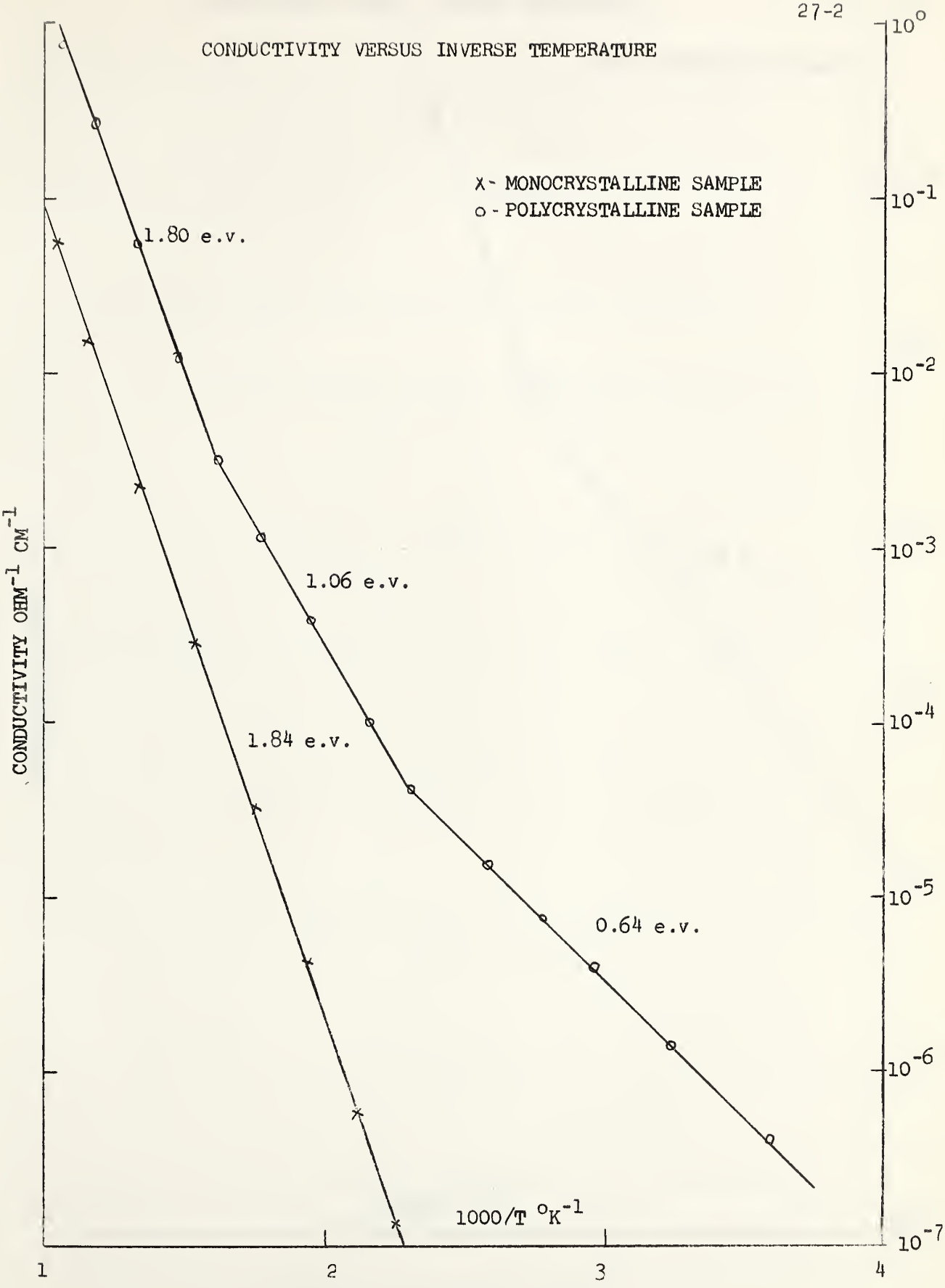

FIGURE 8a: CONDUCTIVITY CURVES

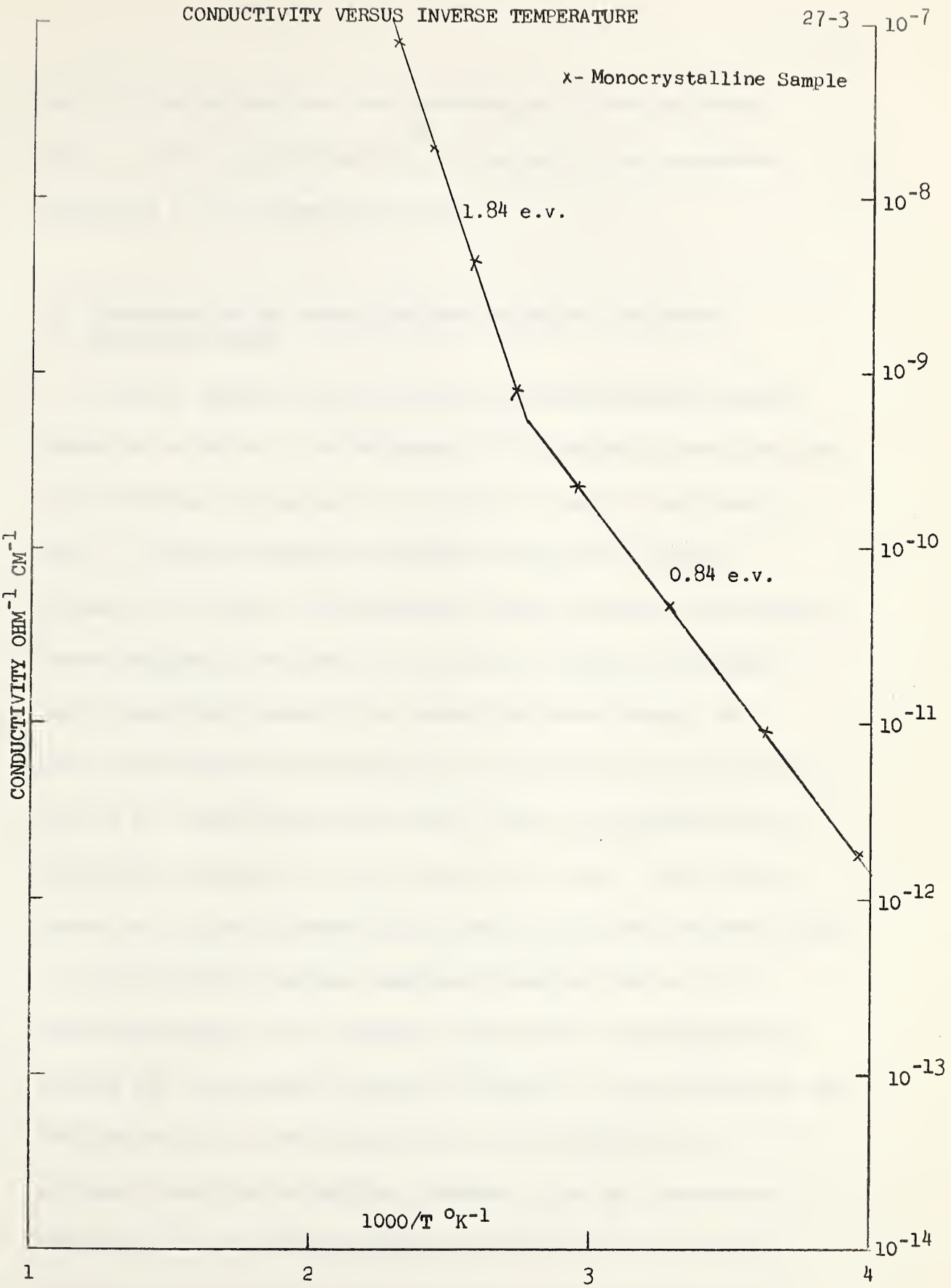

FIGURE 8b: CONDUCTIVITY CURVES

exist in the mid-region of the forbidden gap. This conclusion will be used in conjunction with the analysis of the temperature dependence of the photoconductivity.

B. PHOTOCONDUCTIVITY VERSUS INCIDENT RADIATION WAVELENGTH (RESPONSE CURVES)

Typical response curves for poly and monocrystalline samples installed in holder A, and subjected to the thermal history discussed in conjunction with holder A in Chapter II, page 2, are shown in Fig. 9. They were taken at room temperature and a chopping frequency of 40 cps.. On the basis of Moss' λ_g concept, the response curves indicate a band gap of 1.9 to 2.0 e.v. which is slightly higher than that obtained from conductivity measurements. The peak in the infra-red wavelength region indicates an impurity level about 1 e.v. above the valence bands, which is in agreement with the results obtained from the conductivity curves. The response curves are in good agreement with those of Fortin and Weichman (1962).

Fig. 10 shows the room temperature response curves of a particular sample at two chopping frequencies. Observations were carried out with samples installed in holder A. As can easily be seen the photocurrent in the region from 0.6 to 0.75 microns is extremely sensitive to chopping frequency, with the photocurrent decreasing with increasing chopping frequency. For low chopping frequencies the response curves show two peaks in the visible

wavelength region, one at 0.58 microns and one at 0.66 microns. The 0.66 micron peak disappears with increasing chopping frequency leaving some residual photocurrent indicating that in this region the photoresponse is due to two processes, one fast, one slow, as postulated in Chapter III. These response curves may be interpreted as follows. The peak at 0.58 microns arises from band to band transitions and on the basis of Moss' $\lambda_{\frac{1}{2}}$ concept, indicates a band gap of about 2 e.v., while the peak at 0.66 microns arises from transitions involving a low lying impurity level and indicates that this level lies about 0.25 e.v. above the valence band.

At room temperature a detailed examination of the dependence of the photocurrent on chopping frequency was carried out for an incident radiation wavelength of 0.64 microns. Firstly, the photocurrent was measured as a function of time, with t = 0 at the time of initial illumination. It was found that an equation of the form;

$I = K + A(1-\exp(-t/T_R^A))$, with I as the photocurrent, represents the observations. These results are shown in Fig.11, and a value for T_R^A of 23 milliseconds is obtained. Using this value of T_R^A and the observed data of photocurrent versus chopping frequency, it was found that equation (28),(Chapter III, page 23) was representative of the data as shown on Fig. 12. A value for the decay time of 70 milliseconds was found. Although the rise and decay times are different, Fig. 13 shows a plot of the photocurrent versus chopping time which indicates that equation (31) is valid for

these observations with a response time of 40 milliseconds. Although the assumption of equal rise and decay times is invalid, it does not invalidate equation (31). Equation (31) may be obtained by assuming that some type of mean response time may be used to characterize the photocurrents dependence on time. Fig. 13 then shows that this assumption along with equation (31) is valid for the observations. This data besides showing the character of the time dependence of the photocurrent, substantiates the postulate that competing processes lead to the observed values of the photocurrent.

Fig. 14 shows room temperature response curves taken on samples installed in holder B. Curves numbered by a letter with the suffix 1 were taken at 10 cps. and curves with the suffix 2 were taken at 40 cps.. These curves were taken in the following sequence. After preparation the sample was installed and a high vacuum established. Curves A were then taken. The sample was then annealed at about 300°C under high vacuum and curves B were taken. After subsequent annealing at 1000°C under high vacuum curves C were taken. It can be seen that the first annealing process causes the curves to shift to longer wavelengths and also causes the frequency dependent peak to occur. The second annealing process causes the curves to shift back to the shorter wavelength region and causes the frequency dependent peak to disappear. Curves A and C give band gaps of from 2.3 to 2.6 e.v. which are higher than

previous investigations have ever revealed. Curves B are interpreted as are the curves in Fig. 10, giving a band gap of 1.9 e.v. and an impurity level about 0.25 e.v. above the valence band. Insufficient evidence has been gathered in order to attempt an analysis of this behavior but a possible explanation will be presented. Initially the sample has a surface layer of high percentage oxygen content which is inactive in contributing to the photocurrent. After the first annealing process this oxygen is driven into the sample and becomes active in determining the photocurrent. The second annealing process drives off the major portion of this excess oxygen allowing the photoresponse to return to its initial character. This is compatible with the frequency dependent peak being caused by a high density oxygen impurity level.

It is interesting to note that Fortin (1962) has observed a peak at 0.66 microns which he termed an "extra peak". He observed that this peak disappeared with decreasing temperature. Assuming this peak to be the one discussed above this behavior is easily explained on the basis of a response time that increases with decreasing temperature. From the theory (Chapter III) it is seen that at high temperatures the photocurrent ΔI is given

by $\Delta I = K + A$, at medium temperatures

by $\Delta I = K + \frac{A t_o}{2T_A}$, at low temperatures

by $\Delta I = K$, and thus only the fast process is instrumental in determining the photoresponse in this wavelength region at low

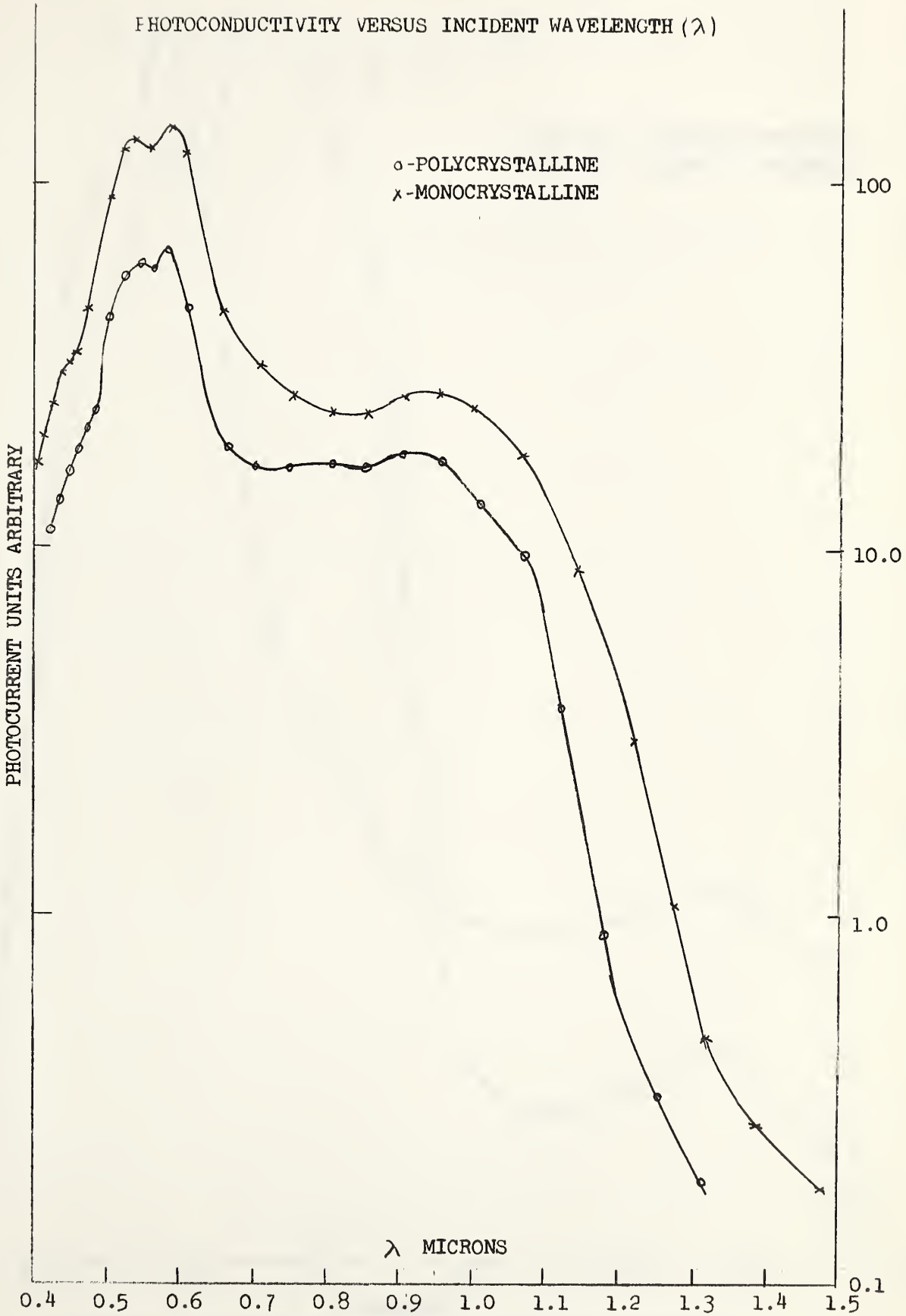

FIGURE 9: RESPONSE CURVES

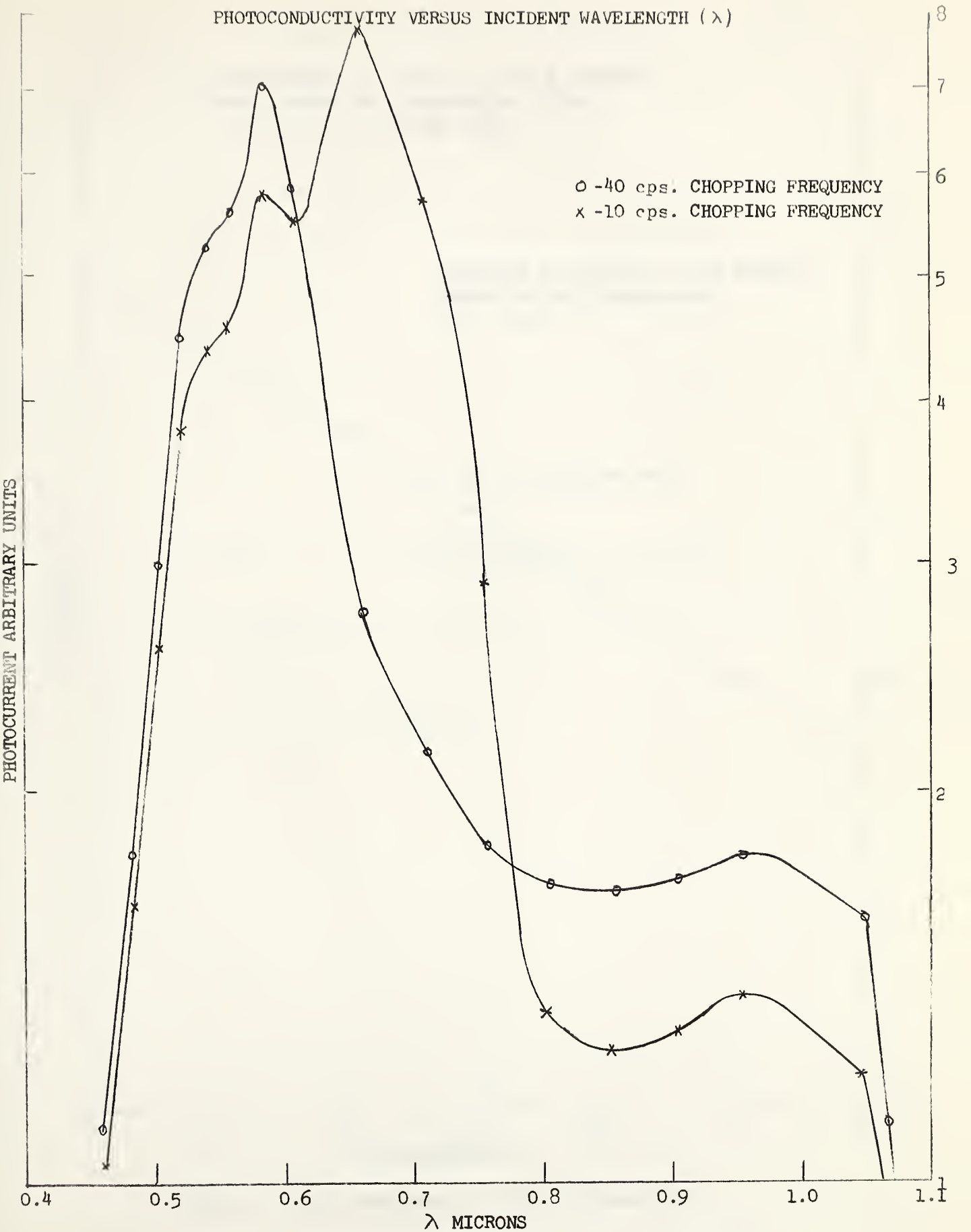

FIGURE 10: RESPONSE CURVES AT TWO CHOPPING FREQUENCIES

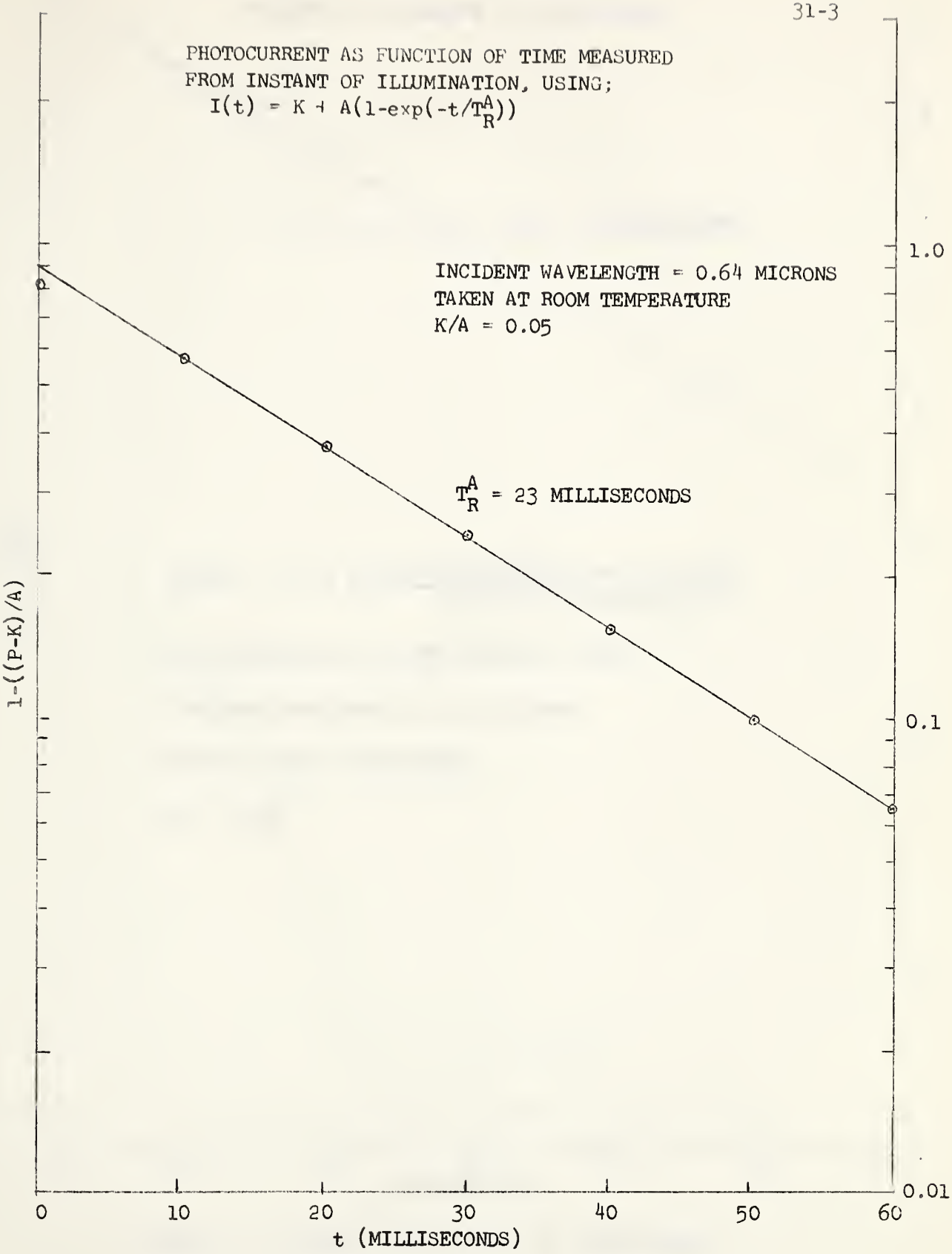

FIGURE 11: TIME DEPENDENCE OF RISING PHOTOCURRENT

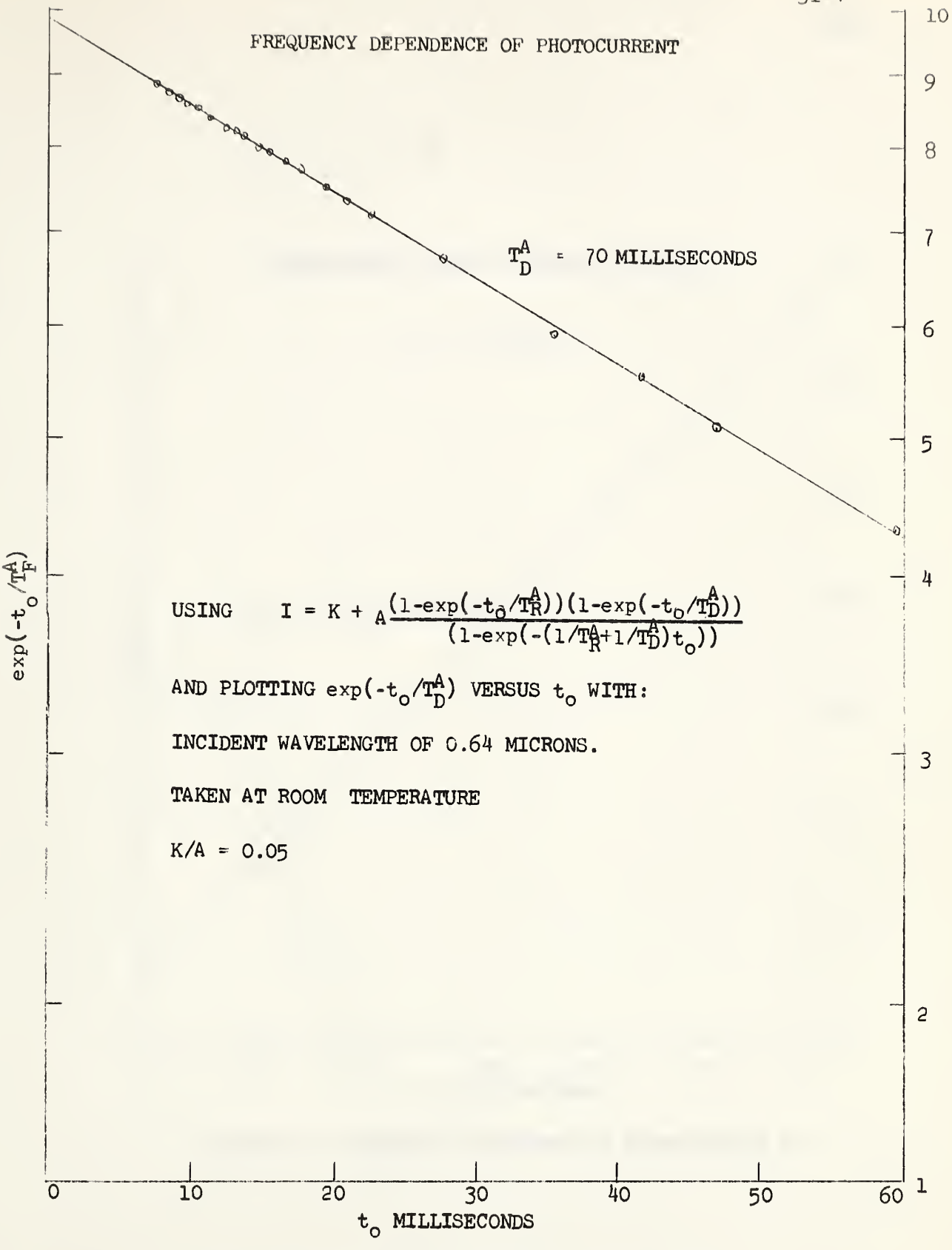

FIGURE 12: FREQUENCY DEPENDENCE OF PHOTOCURRENT I

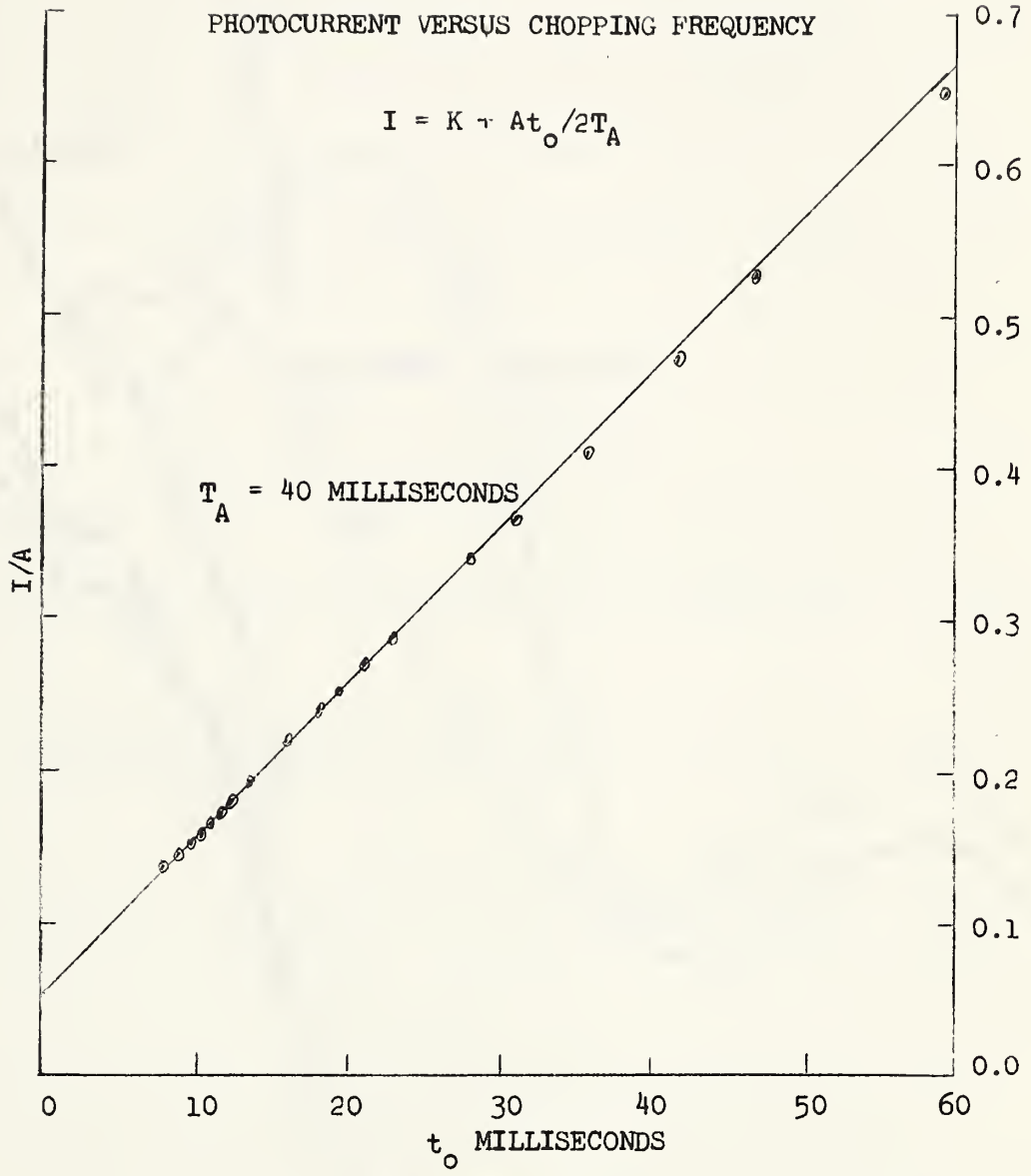

FIGURE 13: FREQUENCY DEPENDENCE OF PHOTOCURRENT II

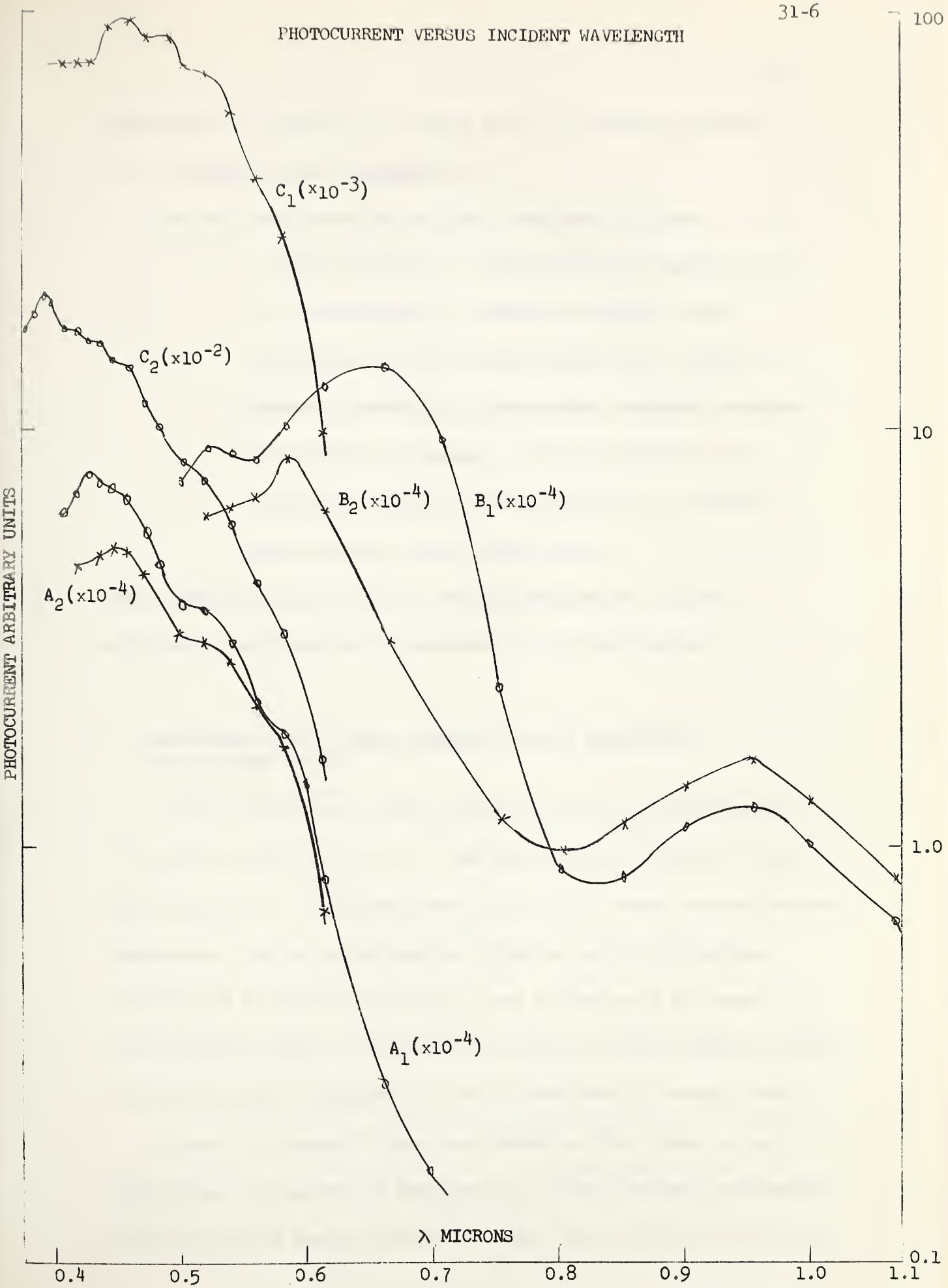

FIGURE 14: EFFECT OF ANNEALING ON RESPONSE CURVES

temperatures. From this it follows that the frequency dependent peak disappears at low temperatures.

The main conclusions to be drawn from these data are:

1. The existence of a dense low lying impurity level.
2. The existence of competing processes being responsible for the photocurrent, one of which is dominant depending on temperature, chopping frequency and incident wavelength. Of course there will be conditions under which these processes contribute about equally to the photocurrent.

These conclusions will also be used in conjunction with the analysis of the temperature dependence of the photocurrent.

C. PHOTOCONDUCTIVITY VERSUS INVERSE ABSOLUTE TEMPERATURE (TEMPERATURE CURVES)

Fortin and Weichman (1962) published results of investigations of the temperature dependence of the photocurrent in cuprous oxide. They found that if log photocurrent was plotted versus inverse absolute temperature, regions of exponential behavior could be discerned. As mentioned in the Introduction, it was on the basis of these investigations that it was decided to carry out a more exhaustive study of the temperature dependence of the photocurrent in cuprous oxide.

Figures 15 through 22 show the results of this study as log photocurrent versus inverse temperature at fixed incident wavelengths for both poly and monocrystalline samples. These curves, which were

taken at a chopping frequency of 40 cps., have been corrected for equal incident intensities at all incident wavelengths in the manner discussed in Chapter II (See page 4). In general it was found that regions of exponential dependence were displayed in which the photocurrent, ΔI, could be expressed as;

$\Delta I \propto \exp(E/kT)$. This equation in conjunction with the data was used to calculate the values of E which are given on the graphs in electron volts. In the following a qualitative analysis of these data, based on a phenomenological theory developed in Chapter III, will be presented. Throughout this discussion "K" will be used to denote the relatively fast process connected with valence band transitions and "A" to denote the relatively slow process connected with the low lying impurity level. Temperature curves labelled "a" represent measurements taken on polycrystalline samples and curves labelled "b" represent measurements taken on monocrystalline samples.(9) A summary of the parameters used in the analysis is given in Table I. Some of the curves are not distinct enough to enable all the parameters to be calculated and in these instances blank spaces have been left. The values of E_2 used in the following analysis are obtained from the conductivity measurements in section A of this chapter.

Fig. 15 shows temperature curves taken at an incident wavelength

(9) For Figures 15 through 22 the inverse temperature scale for the curves labelled "a" is at the bottom of the page and the inverse temperature scale for the curves labelled "b" is on the top of the page.

(E's are in electron volts and temperature in degrees Kelvin)

PARAMETER	$E_2/2-E_{oA}$		E_{oA}		$1000/T_1$		$1000/T_c$		$1000/T_2$		$E_{oA}+E_A$		E_A		$1000/T_3$		$1000/T_4$		E_{oK}	
CURVE / FIG.#	a	b	a	b	a	b	a	b	a	b	a	b	a	b	a	b	a	b	a	b
15 (0.538u)							2.70										3.65	3.65	0.06	0.20
16 (0.584u)	0.27		0.11		2.65		2.75	2.85									3.65	3.70	0.13	0.24
17 (0.640u)	0.33		0.05		2.85		2.90	2.90	3.10		0.19		0.14		3.60		4.20	3.65	0.12	0.22
18 (0.706u)	0.47		-0.09		2.80		2.95		3.10		0.29		0.38		3.40		4.35	3.70	0.14	0.24
19 (0.804u)	0.20	0.31	0.18	0.37	3.10	3.20	3.60	3.50									4.60	3.70	0.16	0.22
20 (0.904u)	0.25	0.30	0.13	0.38	3.10	3.20	3.50	3.40									4.00	3.65	0.20	0.23
21 (1.004u)	0.22	0.29	0.16	0.39	3.10	3.20	3.45	3.35									3.65	3.65	0.19	0.25
22 (1.116u)	0.19	0.26	0.19	0.42	3.05	3.15	3.40	3.30									3.90	3.50	0.24	0.23

TABLE I

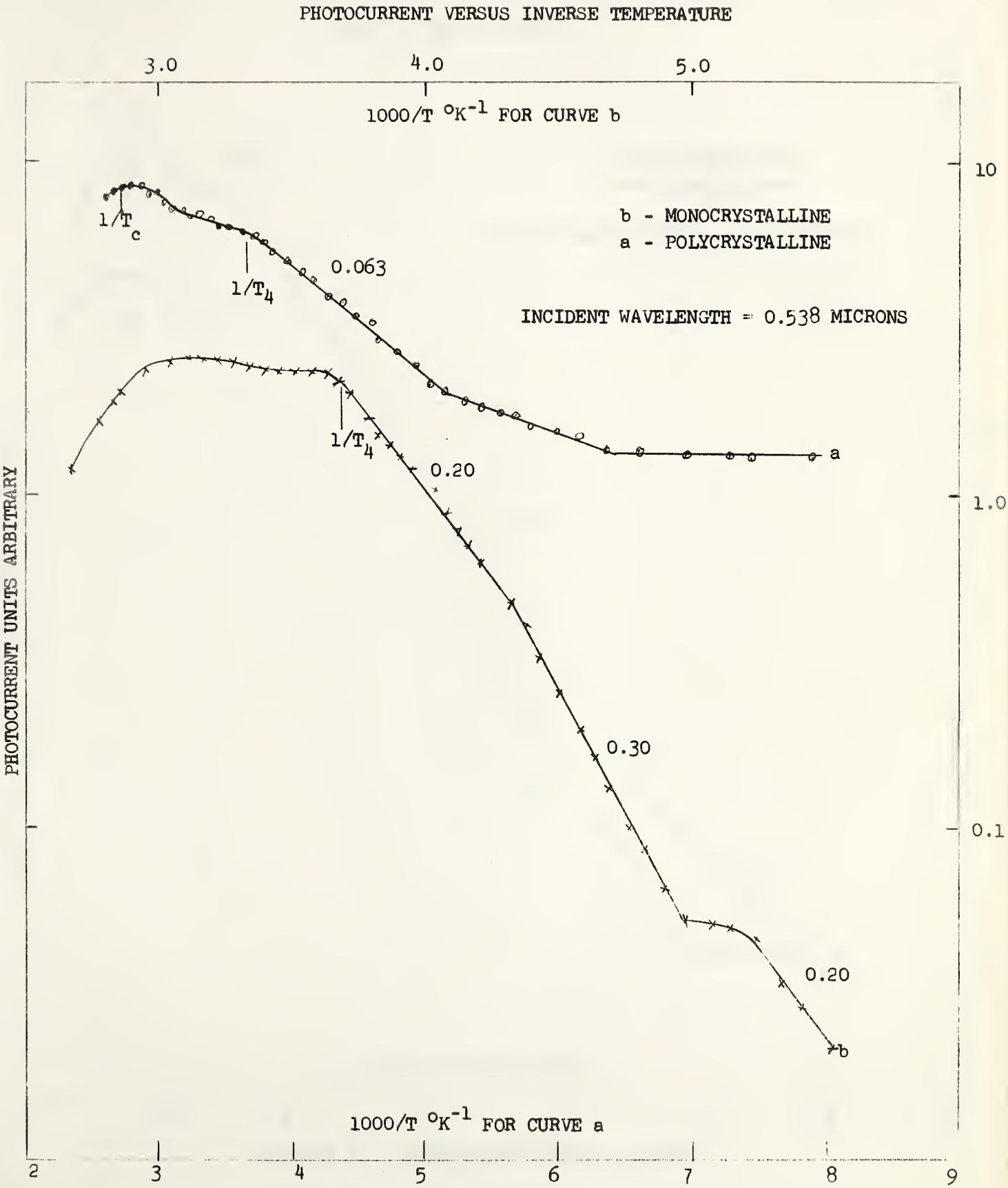

FIGURE 15: TEMPERATURE CURVES (0.538 u)

PHOTOCURRENT VERSUS INVERSE TEMPERATURE

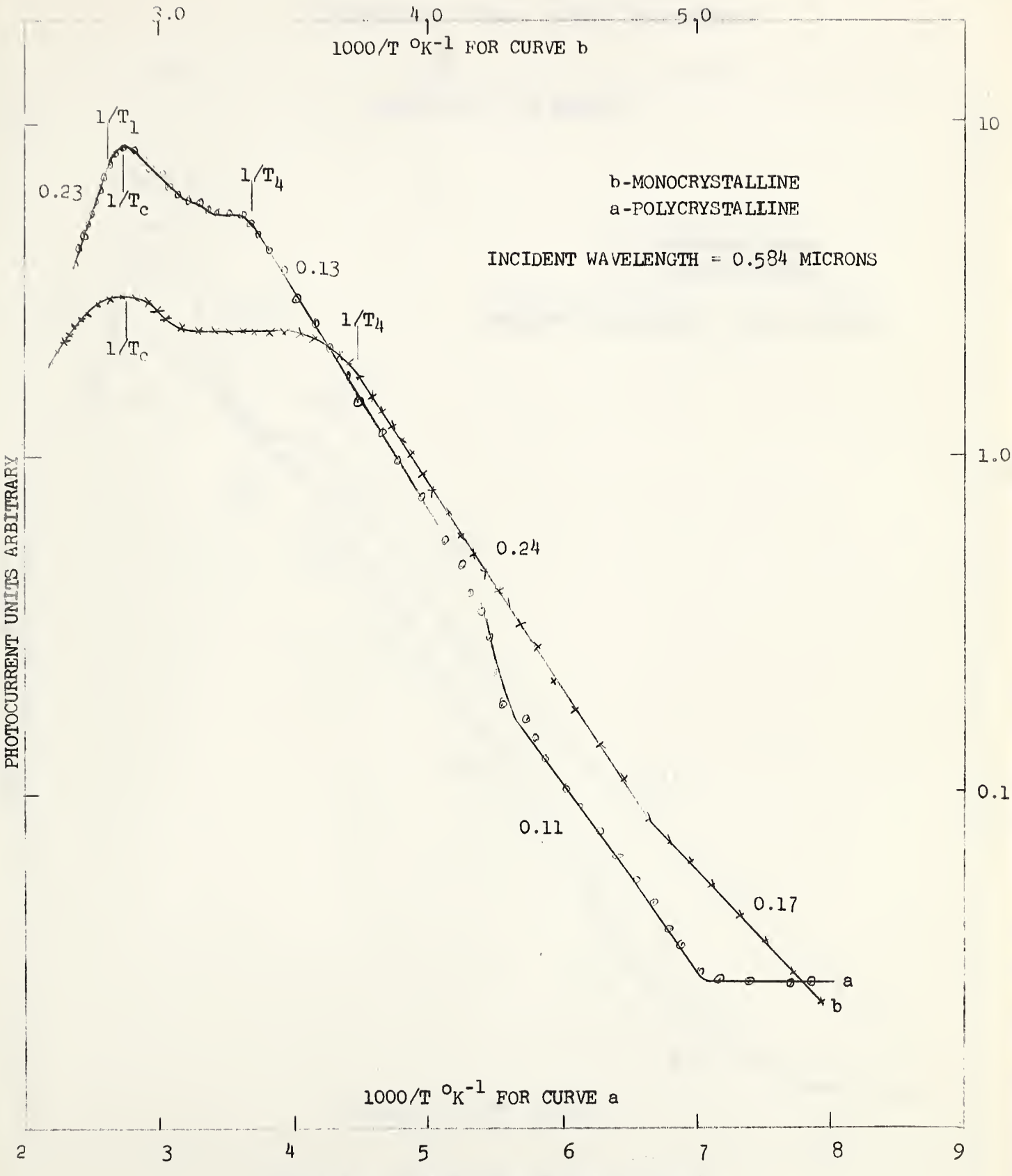

FIGURE 16: TEMPERATURE CURVES (0.584u)

PHOTOCURRENT VERSUS INVERSE TEMPERATURE

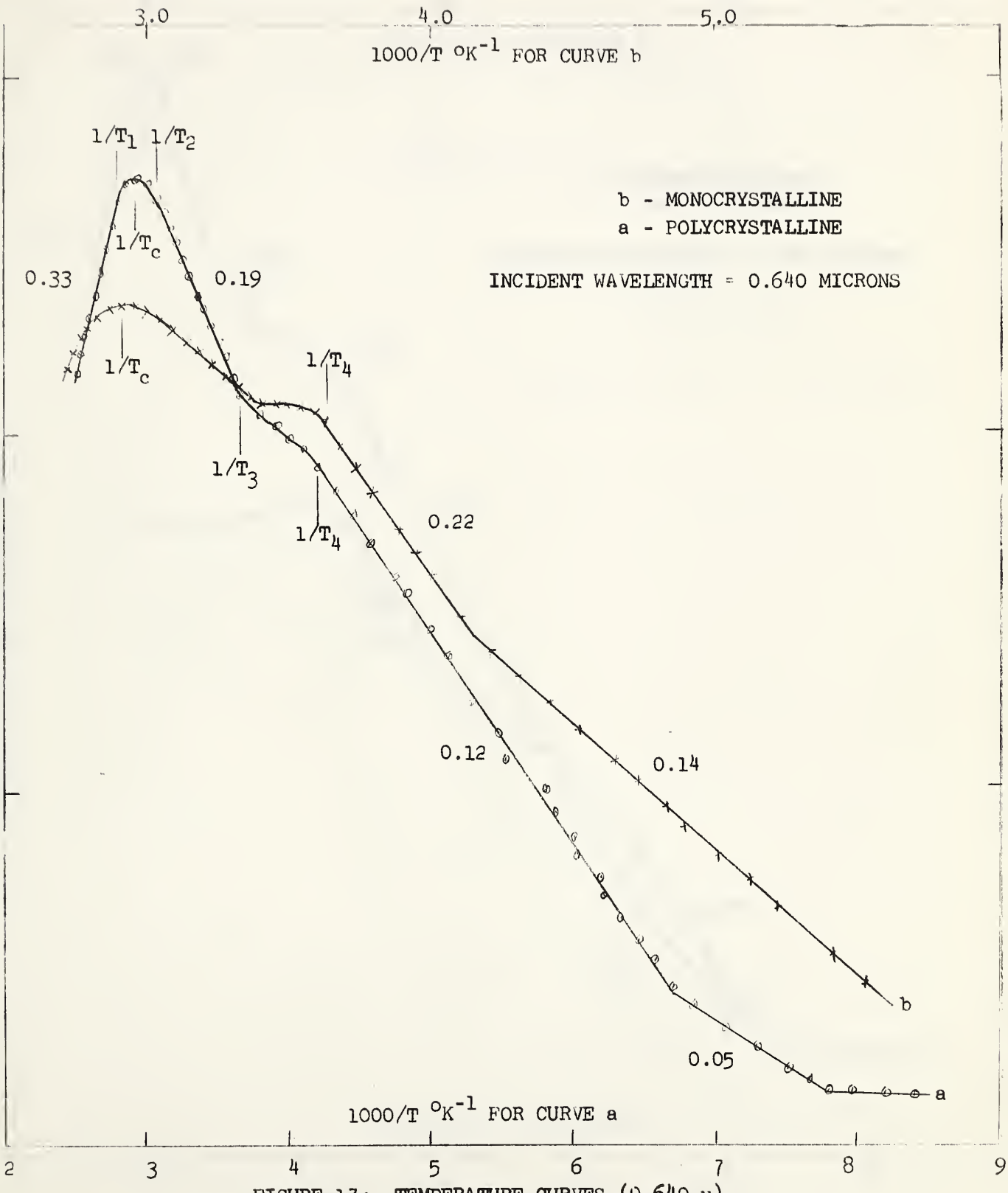

FIGURE 17: TEMPERATURE CURVES (0.640 u)

PHOTOCURRENT VERSUS INVERSE TEMPERATURE

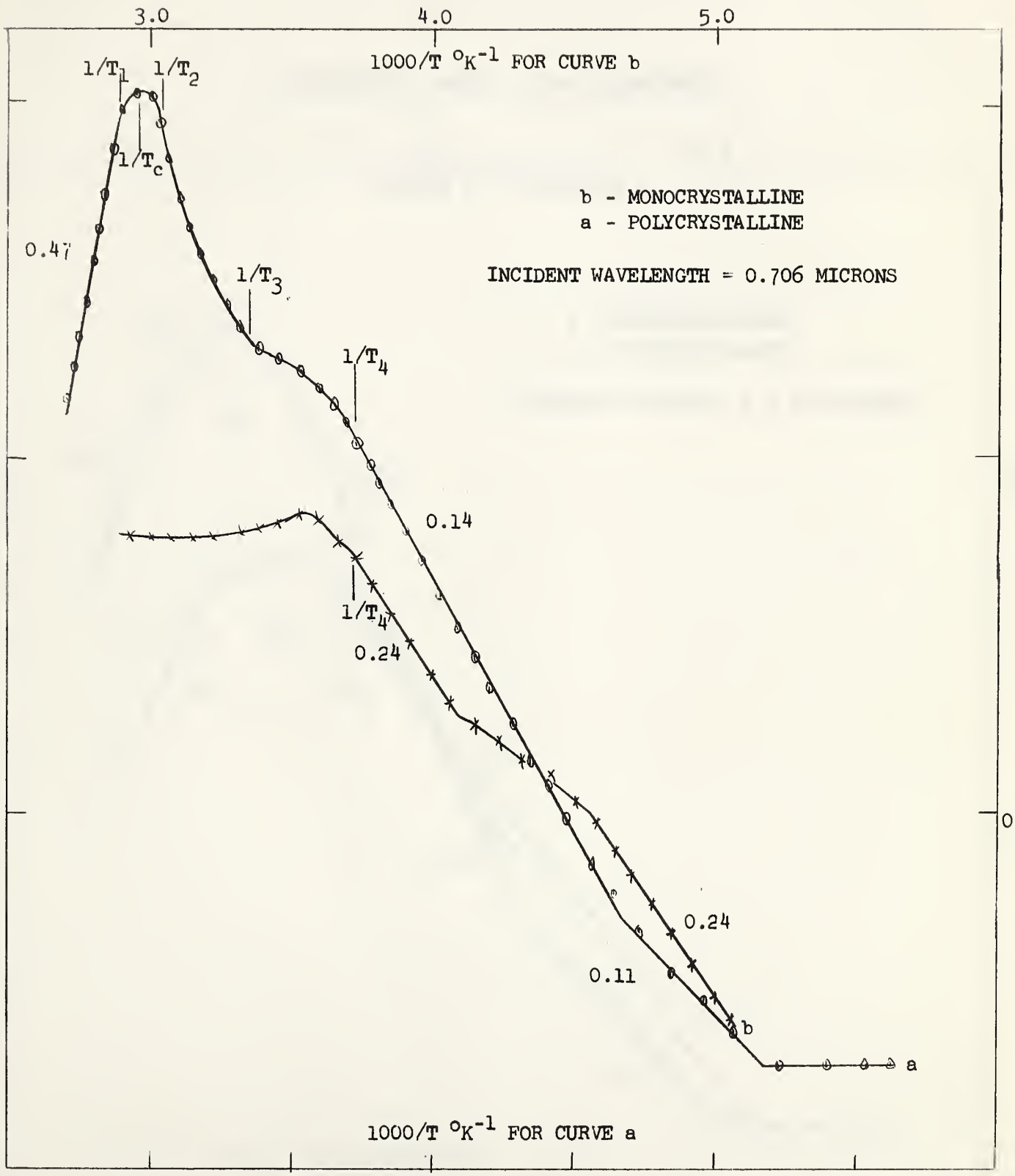

FIGURE 18: TEMPERATURE CURVES (0.706 u)

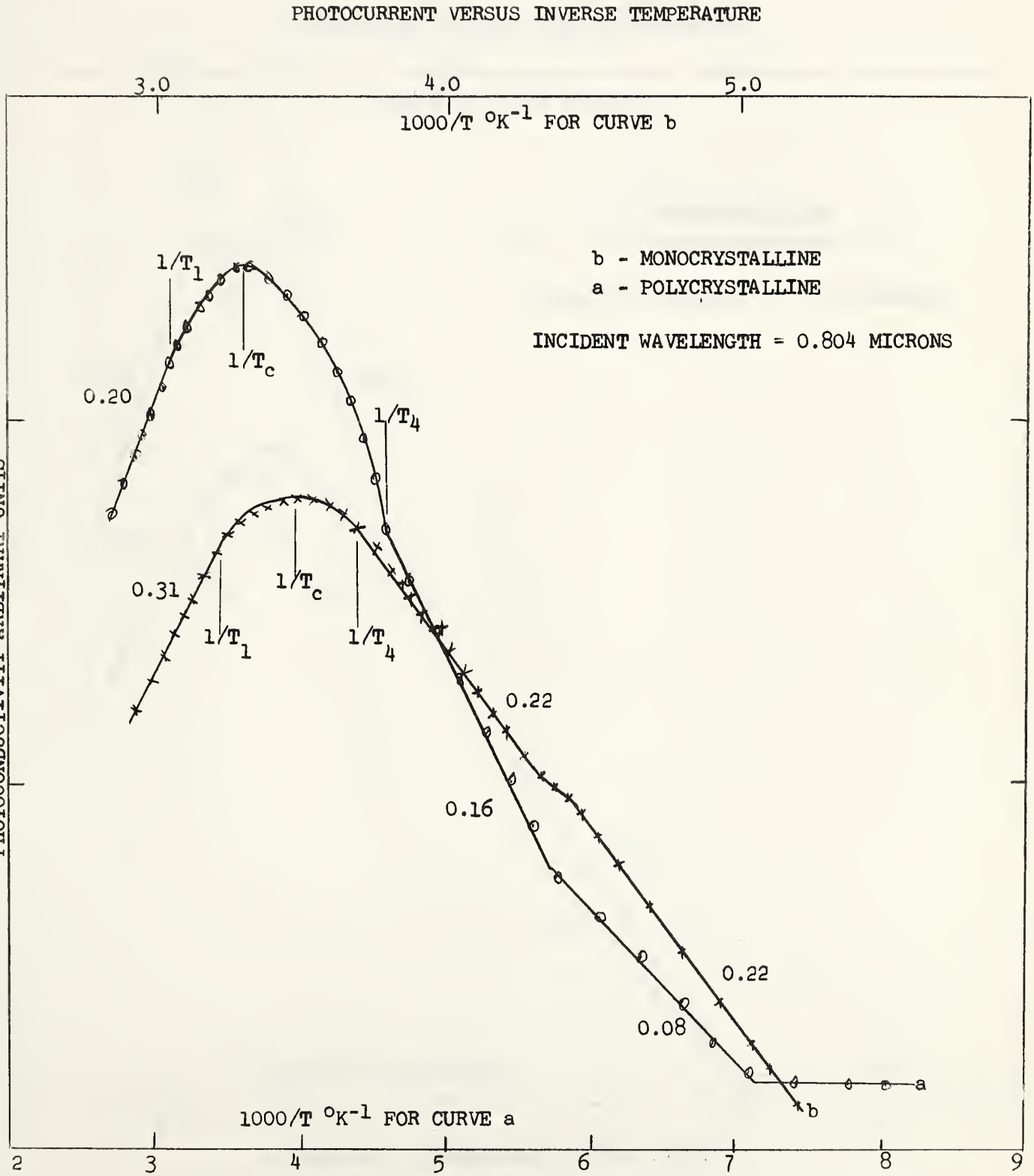

FIGURE 19: TEMPERATURE CURVES (0.804 u)

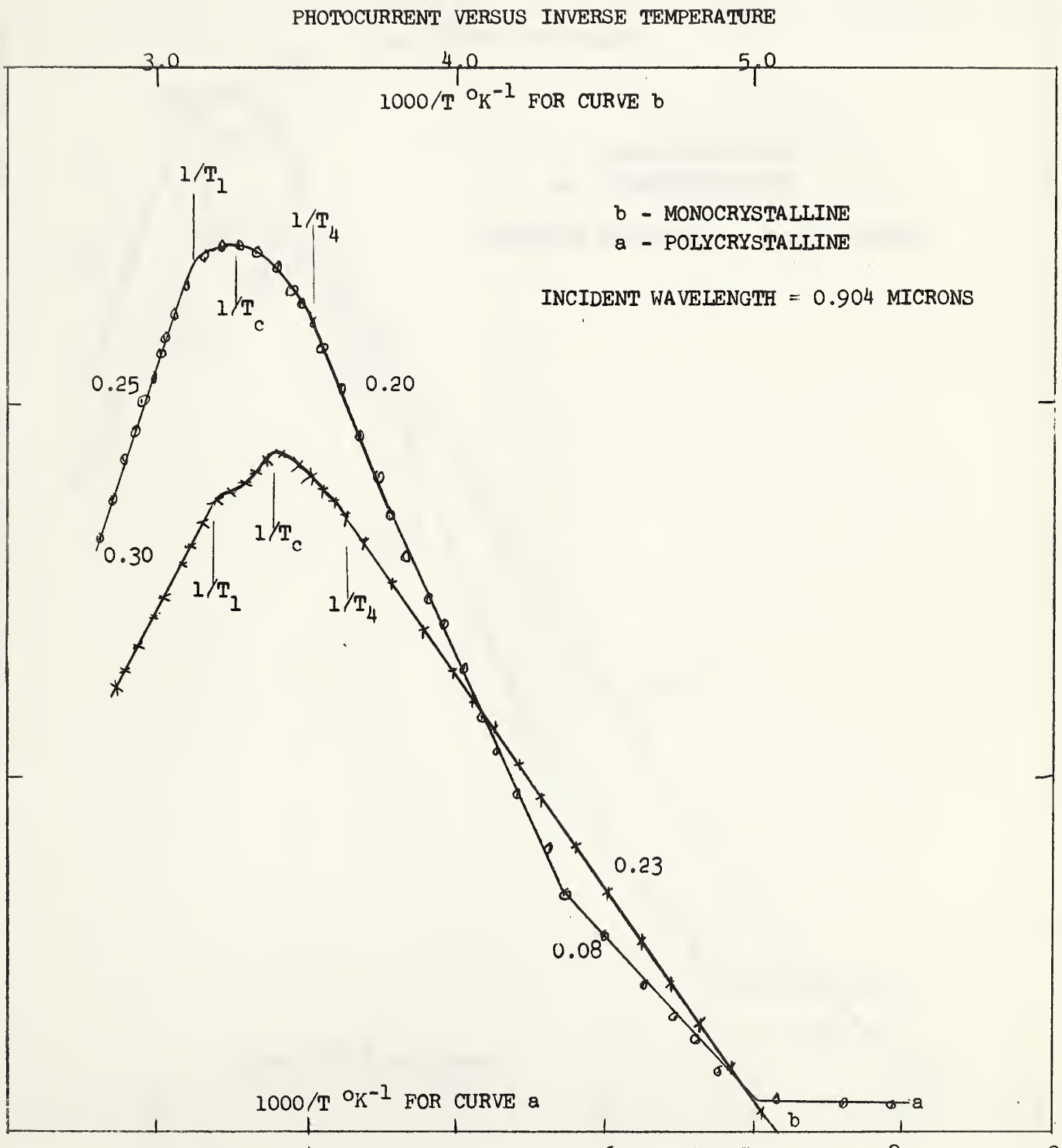

FIGURE 20: TEMPERATURE CURVES (0.904 u)

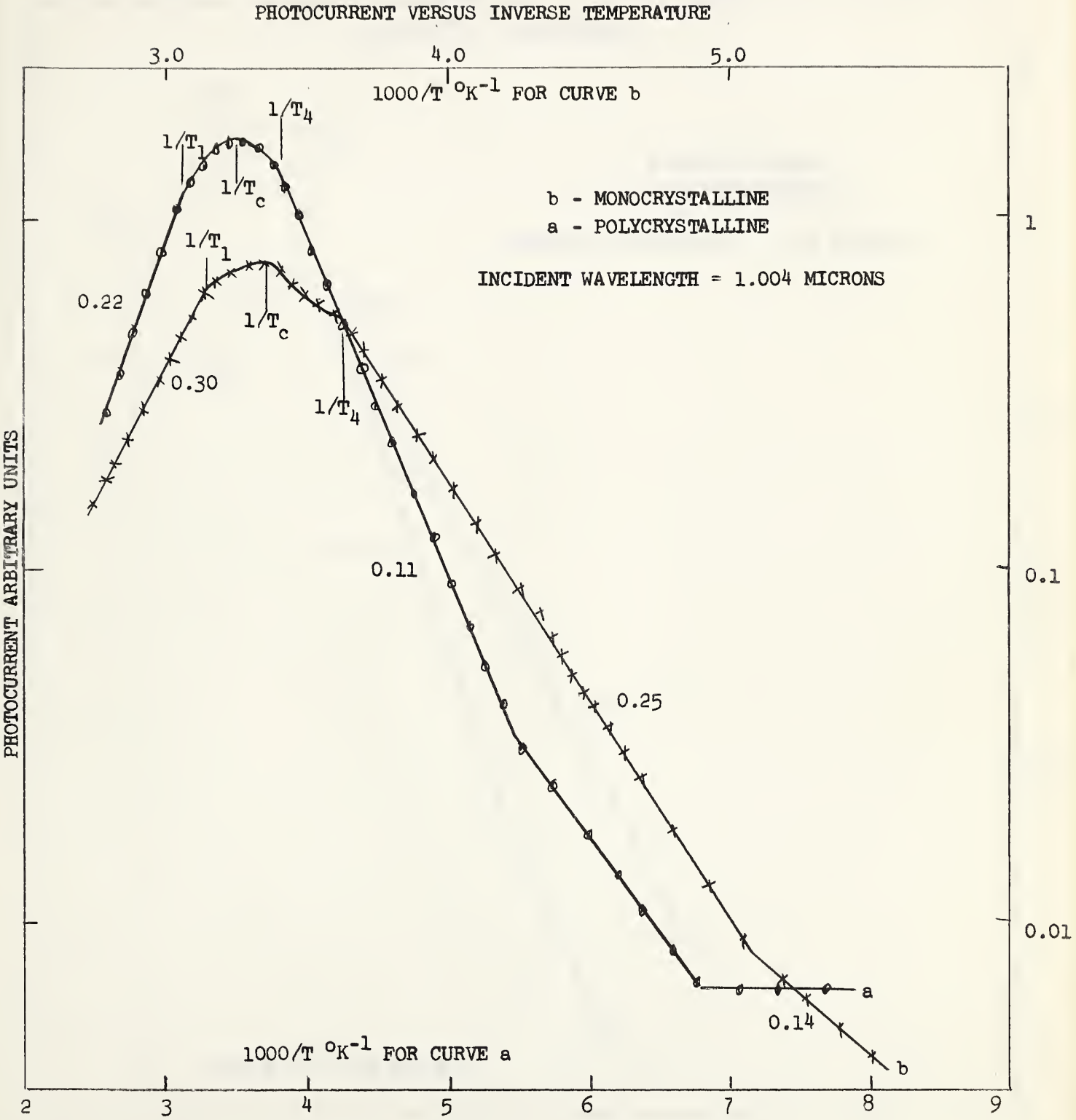

FIGURE 21: TEMPERATURE CURVES (1.004u)

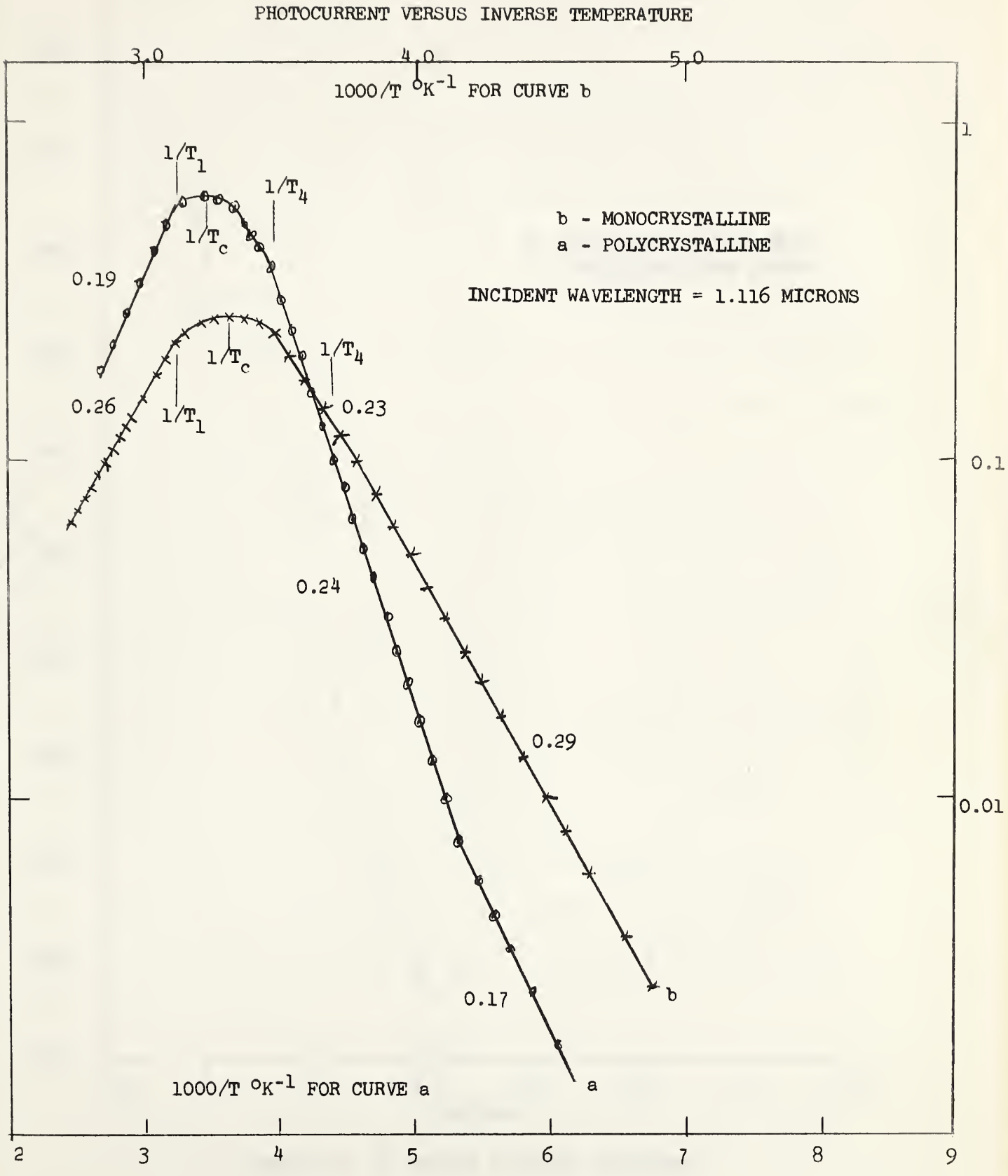

FIGURE 22: TEMPERATURE CURVES (1.116u)

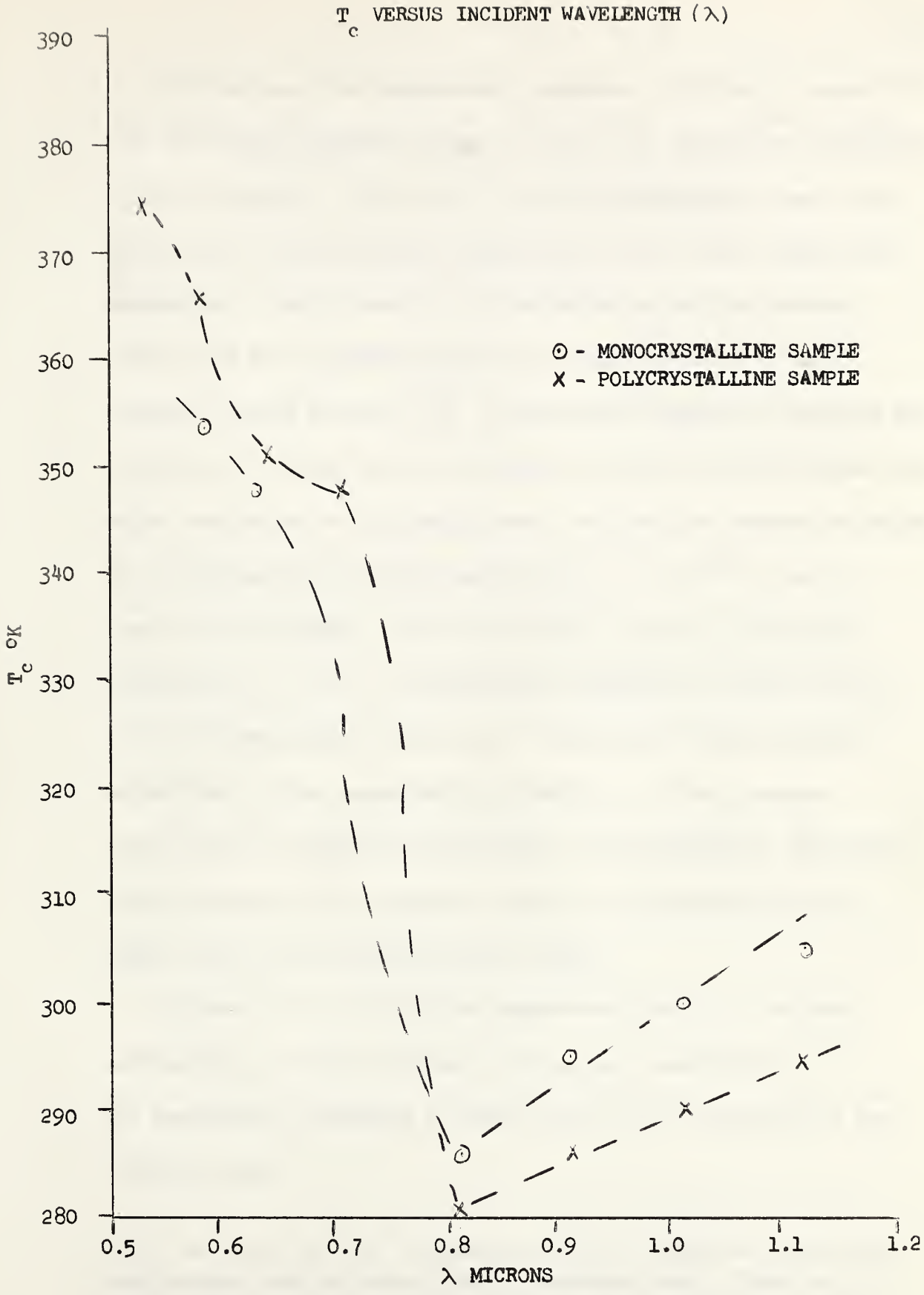

FIGURE 23: T_c VERSUS INCIDENT WAVELENGTH

of 0.538 microns. The temperature dependence exhibited by curve "a" over the whole temperature range is due to the temperature dependence of the K process. For curve "b" the high temperature rise in the photocurrent with decreasing temperature is due to the temperature dependence of the A process. In the region of the flat portion just before the exponential decrease in the photocurrent the A process is being cut out (10). With further temperature decrease the A process is cut out to such an extent that the K process becomes the major contributor to the photocurrent and thus the temperature dependence of the photocurrent in this region ($1/T \quad 3.7 \times 10^{-3}$) is due to that of the K process. In the temperature region of $1/T$ greater than about 3.7×10^{-3}, the temperature dependence of both curves is due to the temperature dependence of the ratio of the excitation probability to the recombination probability of the K process (neglecting the temperature dependence of the mobility). Thus this ratio decreases with temperature faster for the monocrystalline sample than for the polycrystalline sample.

Figures 16, 17 and 18 show temperature curves for incident wavelengths of 0.584, 0.64 and 0.706 microns respectively. The temperature dependence of these curves will be analyzed on the following basis.

(10) The term "cut out" is used to refer to conditions under which the response time is slower than the chopping time. Thus for A.C. measurements the total possible response due to the slow response time process is not measured.

Consider decreasing temperature and processes A and K such that A is greater than K. At high temperatures the A process dominates and has a response time shorter than the chopping time. In this region the temperature dependence may be written from equation (10), page 17, using the conditions;

$$\frac{u^{RA}}{D_A} \propto \exp(-E_{oA}/kT)$$

$$P_o >> M_A$$

$$P_o = A_2 E(-E_2/2kT)$$

as;

Region 1: $1/T_1 > 1/T$; $\quad I \propto \exp((E_2/2 - E_{oA})/kT)$.

The photocurrent then reaches a maximum before the response time becomes of the order of the chopping time, giving the transition region with the temperature at which the photocurrent is a maximum, T_c, given by;

Region 2: $1/T_1 < 1/T < 1/T_2$; $\quad T_c = \dfrac{E_2}{2k\,\mathrm{Ln}((E_2/2 - E_{oA})A_2/E_2 M_A)}$.

Then the chopping time becomes much smaller than the response time and the photocurrent decreases exponentially as;

Region 3: $1/T_2 < 1/T < 1/T_3$; $\quad I \propto \exp(-(E_{oA} + E_A)/kT)$.

Then a sufficient amount of the photocurrent due to the slow process gets cut out such that;

Region 4: $1/T_3 < 1/T < 1/T_4$; $\quad I = K + A \dfrac{t_o}{2T_{oA}} \exp(-E_A/kT)$

with the two terms of the same order of magnitude giving rise to a so called transition region. Further decrease in temperature is sufficient to completely cut out the slow process giving rise to the

photocurrents' temperature dependence as;

Region 5: $1/T_4 < 1/T$; $\quad I = K \propto \exp(-E_{oK}/kT)$

in the approximation that $\frac{uR_K}{D_K} \propto \exp(-E_{oK}/kT)$

and $M_K >> P_o$.

Table I shows the values of the parameters postulated above. From this table it can be seen that E_{oA} can be either negative or positive. A positive value for E_{oA} indicates that the ratio of excitation probability to recombination probability for the A process is a decreasing function of inverse temperature, while a negative value indicates that this ratio is an increasing function of inverse temperature. It is also noted that E_{oK} is positive indicating that for the K process the ratio of the excitation probability to the recombination probability is an increasing function of inverse temperature.

Figures 19 through 22 show the temperature curves for incident wavelengths of 0.804, 0.904, 1.004 and 1.116 microns respectively.

The analysis of these curves is based on the following concept. As in Chapter III, it is assumed that the photocurrent due to the A process is given by;

$(\frac{uR_A}{D_A})/(M_A + P_o)$, and the photocurrent due to the K process is given by;

$(\frac{uR_K}{D_K})/(M_K + P_o)$, where the symbols have the same meaning as in Chapter III. The conditions;

$$\frac{uR_A}{D_A} \propto \exp(-E_{oA}/kT)$$

and $\frac{\mu_K}{D_K} \propto \exp(-E_{oK}/kT)$, are assumed to prevail. At high temperatures the A process is dominant and it is assumed as before that $P_o >> M_A$. With $P_o \propto \exp(-E_2/2kT)$, the photocurrent, ΔI rises exponentially as;

Region 1: $1/T < 1/T_1$; $\Delta I \propto \exp(E_2/2 - E_{oA})/kT$.

Then a region in which M_A is in the order of P_o occurs giving rise to a maximum in the photocurrent at a temperature given by;

Region 2: $$T_c = \frac{E_2}{2k\mathrm{Ln}((E_2/2 - E_{oA})A_2/E_2M_A)} .$$

Just past this peak the response of the A process becomes quite slow and thus is cut out, leaving the photocurrent due to the K process. In this low temperature region M_K is much less than P_o and the photocurrent is given by;

Region 3: $1/T > 1/T_4$; $I \propto \exp(-E_{oK}/kT)$.

For high temperatures the exponential increase in photocurrent is attributed to the temperature dependence of the A process, thus giving values for $E_2/2 - E_{oA}$ as shown in Table I. The peak is assumed to arise due to conditions discussed in Chapter III and values of T_c, (the temperature at which the maximum photocurrent occurs), are given in Table I. Just past this peak on the low temperature side, the A process is cut out and the subsequent exponential decrease in the photocurrent is attributed to the temperature dependence of the K process, giving values of E_{oK} shown on Table I. It is seen that both E_{oA} and E_{oK} are positive indicating that for both processes the ratio of the excitation probability to the

recombination probability is a decreasing function of inverse temperature. E_{oA} and E_{oK} do not show much variation with incident wavelength. If any variation is present, the data indicates a trend towards larger values for increasing incident wavelength.

Fig. 23 shows a plot of the temperature at which the photocurrent is a maximum versus incident wavelength. According to theory, this temperature is given by;

$$T_c = E_2/2k\mathrm{Ln}((E_2/2-E_{oA})A_2/E_2M_A) \ .$$

It is seen that for a wavelength of about 0.75 microns a definite break in the curves occurs. For incident wavelengths less than 0.75 microns, the temperature at which the photocurrent is a maximum is in the region of 340°K to 370°K. For incident wavelengths greater than 0.75 microns the temperature at which the photocurrent is a maximum occurs in the region of 280°K to 300°K. For short wavelengths the photocurrent is dependent on transitions involving the conduction band, while for long wavelengths the photocurrent is not dependent on transitions involving the conduction band. It is in the incident wavelength region of about 0.75 microns that the processes leading to the photocurrent are changing character. Although this may be coincidental, it would appear that the break in the curves, shown on Fig. 23, is associated with a changeover in the type of process leading to the photocurrent. On this basis, and using the equation for T_c, the break must be associated with a sudden

change in M_A and E_{oA} as the incident wavelength changes from values just less than 0.75 microns to values just greater than 0.75 microns.

It is interesting to note that Niekisch (1951), gives data on the variation of the photocurrent in CdS (Cadmium Sulfide) with temperature, which show a maximum in the photocurrent. His data give values of T_c that, plotted versus incident wavelength, show a break at about 0.49 microns.

CHAPTER V: CONCLUSION

Experiments were conducted to determine the temperature dependence of the photoconductivity of high resistivity poly and mono-crystalline cuprous oxide. The results have been presented in graphic form and analyzed on the basis of the theory previously developed.

Conductivity and response curves were obtained in order to characterize the samples. It was found that the behavior of the samples investigated was essentially the same as that described by previous investigators. These data are interpreted as meaning: a band gap of about 2 e.v.; a relatively high density oxygen impurity level lying about 0.25 e.v. above the valence band; and a relatively low density impurity level lying in the region of 0.8 e.v. to 1.4 e.v. above the valence band. It was also substantiated that two competing processes, one fast (K) and one slow (A) are present under all conditions of investigation. The slow process is associated with transitions involving the high density, low lying, oxygen impurity level, and the fast process is associated with the valence band.

The phenomenological theory was used to analyze the data on the dependence of the photocurrent on temperature.

The analysis of the temperature curves is based in part on the two parameters, R_A/D_A, and R_K/D_K (the ratios of the excitation probability to the recombination probability for the slow and fast processes respectively). It was found that the temperature

dependence of these parameters may be represented as;

$$R_A/D_A \propto \exp(-E_{oA}/kT)$$

and $$R_K/D_K \propto \exp(-E_{oK}/kT).$$

The dependence of these ratios on wavelength occurs through the parameters E_{oA} and E_{oK} . The observed values of E_{oA} and E_{oK} are shown in Table I. There is little variation in E_{oK} for the incident wavelengths investigated. For the monocrystalline sample, E_{oK} shows only a mean variation of 10% from 0.226 e.v., while for the polycrystalline sample there is a trend for lower values (about 0.11 e.v.) at wavelengths less than about 0.75 microns and higher values (about 0.20 e.v.) at wavelengths greater than about 0.75 microns. E_{oA} for the polycrystalline sample is also smaller (about 0.08 e.v.) for wavelengths less than 0.75 microns than for longer wavelengths (about 0.16 e.v.). The values of E_{oA} for the monocrystalline sample are not clear from the graphs for the shorter wavelengths, but the indication is that the variance in E_{oA} over the wavelengths of investigation is less than about 10% from the mean of 0.38 e.v.. From the consistency of the values of E_{oA} and E_{oK}, it is tempting to make an association of these values with the above proposed energy level spacing. The ratios of excitation probability to recombination probability for these processes should depend upon the energy level spacing, but the manner in which this dependence would affect the temperature dependence of these ratios is not clear. An examination of the basic

theory of transitions for the model under discussion would be needed in order to determine this association. Only one negative value for E_{oA} is apparent. This may be attributed to an error in the observations or it may be that for this incident wavelength E_{oA} is negative in the high temperature range, changing to a positive value at lower temperatures. In general it may be concluded that the ratio of excitation probability to recombination probability for the incident wavelengths under investigation is a decreasing function of inverse temperature for both the fast and slow processes.

It is also observed that the temperature curves display a maximum. This maximum, according to theory should be given as;

$$T_c = (E_2)/(2k\mathrm{Ln}((E_2/2-E_{oA})A_2/E_2M_A)),$$

and thus the variation of T_c with incident wavelength should occur due to the variation of E_{oA} and M_A (apparent density of recombination states). Taking the ratio of this equation for incident wavelengths of 0.706 and 0.804 microns gives the ratio of M_A for an incident wavelength of 0.706 microns to M_A for an incident wavelength of 0.804 microns as about one order of magnitude and thus the density of recombination states at wavelengths less than 0.75 microns is greater than that for incident wavelengths greater than 0.75 microns. The dependence of T_c on incident wavelength is shown in Fig. 23 and the break in the curve at about 0.75 microns is taken to signify the point at which the processes leading to the photocurrent change their character.

A more detailed examination of the basic mechanisms of

photoconduction in Cu_2O could be obtained if separate data on the temperature dependence of the excitation probability and recombination probability could be obtained for a number of fixed wavelengths, and this data then combined with data on the temperature dependence of the photocurrent. In its most valuable form data on the temperature dependence of the photocurrent would be; D.C. measurements along with A.C. measurements of a type which would cut out the slow process at all temperatures. These A.C. measurements could be obtained by varying the chopping frequency at each temperature of measurement to an appropriate value determined by monitoring the output signal from the apparatus (discussed above) on an oscilloscope.

The analysis of the results obtained from this study indicates that deeper insight into the mechanisms of photoconduction can be obtained from measurements of the type performed. Although the results only qualitatively substantiate the phenomenological theory developed in the text of this thesis, there is good indication that further study along these lines may give more understanding of the basic mechanisms of photoconduction.

BIBLIOGRAPHY

Bloem, J. Philips Research Reports. 13, 167-193 (1958).

Bube, R.H.. J. Phys. Chem. Solids. 1, 234 (1956-1957)

Dekker, A.J.. Solid State Physics. Prentice Hall, Inc.; N.J. (1957)

Fortin, E.R.. Thesis: Photoconductivity of Monocrystalline Cuprous Oxide; University of Alberta, April 1962 (unpublished).

Fortin, E. and Weichman, F. Canadian J. of Phys. 40, 1703 (1962).

Garlick, J.F.G. Ency. of Phys. 19, 377 (1956).

Kittel, C. Introduction to Solid State Physics. John Wiley and Sons, Inc. N.Y. (1960).

Moss, T.S. Photoconductivity In the Elements. Academic Press Inc. N.Y. (1952).

Mott, N.F. and Gurney, R.W. Electronic Processes in Ionic Crystals, 156 Oxford at the Clarendon Press (1940).

Niekisch, V.E.A. Anna der Physik 8-9, 291 (1950-1951) .

O'Keefe, M. and Moore, W.J. J. Chem Phys 35, 1324 (1961).

Rose, A. Photoconductivity Conference, 3. John Wiley and Sons. N.Y. (1954).

Rose A. ed. Levinston. Photoconductivity, 1. Pergamon Press (1962).

Tauc, J. Photo andThermoelectric Effects in Semiconductors. Pergamon Press N.Y. (1962).

Weichman, F.L. Thesis: The electrical and Optical Properties of Cu_2O; Northwestern U., June 1959 (unpublished).